

ENGINEERING RESEARCH INSTITUTE
UNIVERSITY OF MICHIGAN
ANN ARBOR

TECHNICAL REPORT NO. 2

THE INFRARED SPECTRUM OF CRYSTALLINE
BRUCITE ($\text{Mg}(\text{OH})_2$)

by

R. T. MARA

Project M957

SIGNAL CORPS, DEPARTMENT OF THE ARMY
CONTRACT DA 36-039 sc-5581, SC PROJECT 152B-0, DA PROJECT 3-99-15-022
SQUIER SIGNAL LABORATORY, FORT MONMOUTH, N. J.

September 1954

PREFACE

The following text has been approved as a dissertation for the doctorate at the University of Michigan. Since the author has derived full financial support for this work from a Signal Corps Contract in stipend and funds for equipment, the full account of the work is being submitted as a report to the Signal Corps.

The author is indebted to the many members of the Physics Department, who have been generous with their time and their talents, and appreciation is extended to his fellow workers in infrared for the many stimulating and enlightening discussions. The author is pleased to acknowledge his particular gratitude to Professor G. B. B. M. Sutherland for suggesting the problem and for his invaluable advice and patient encouragement throughout the entire course of the work.

In addition, grateful acknowledgement is made to the following:

Professor E. W. Heinrich and Dr. A. Levinson of the Mineralogy Department for kindly lending the fine brucite crystal samples from the Mineralogical Collections.

Professor R. W. Parry of the Chemistry Department for supplying the compound $\text{Mg}(\text{OD})_2$.

Mr. P. Weyrich for his help and advice on infrared techniques and instrumentation.

ENGINEERING RESEARCH INSTITUTE • UNIVERSITY OF MICHIGAN

Mr. H. Roemer and his associates in the Physics Instrument Shop for their valuable assistance in the design and construction of equipment.

Mr. A. Dockrill for contributing his many talents in the shop and in the laboratory.

TABLE OF CONTENTS

Preface	ii
List of Tables	vi
List of Illustrations	vii
Introduction	1
Chapter 1: REVIEW OF PREVIOUS WORK	4
1.1 General Properties	4
1.2 X-ray Diffraction Studies	6
1.3 Infrared Studies	10
Chapter 2: APPARATUS AND EXPERIMENTAL PROCEDURES	24
2.1 Infrared Spectrometers	24
2.2 Auxiliary Apparatus	26
2.3 Sample Preparation	32
Chapter 3: EXPERIMENTAL RESULTS OF PRESENT STUDY	38
3.1 Introduction	38
3.2 Preliminary Spectra	41
3.3 Spectra of Brucite, Cleaved Sections and Powder	42
3.4 Spectra of Chemically Prepared Mg(OH) ₂ and Ca(OH) ₂	49
3.5 Spectrum ² of Chemically Prepared Mg(OD) ₂	52
3.6 Brucite Spectrum, Sections Normal to Cleavage Plane	54
3.7 Spectra of Brucite at High and Low Temperatures	59
3.8 Carbonate Impurity in Powdered Samples	65
3.9 Increased Resolution, 2 μ -3.2 μ Region	68
(a) 2 μ to 2.6 μ Region	68
(b) 2.8 μ to 3.2 μ Region	74
(c) 2.6 to 2.8 μ Region	78
3.10 Brucite Spectrum, 15 μ -33 μ Region	81
3.11 Summary	
Chapter 4: DISCUSSION OF EXPERIMENTAL RESULTS	85
4.1 Comparison with Previous Infrared Work	85

4.2	Interpretation of Bands in 2 μ -3.1 μ Complex	88
4.3	Summary	102
Chapter 5:	A SUGGESTED NEW STRUCTURE FOR BRUCITE	104
5.1	Demands on the Structure	104
5.2	Suggested OH Orientations	105
	Bibliography	113

LIST OF TABLES

Table
Number

1	Unit Cell Dimensions of Brucite	9
2	Assignments for Brucite Bands	18
3	Reflectivity of Brucite	23
4	Comparison of $\text{Mg}(\text{OH})_2$ and $\text{Mg}(\text{OD})_2$ Bands	54
5	Intensities of Brucite Bands at 30°C and 350°C	61
6	Intensities of Brucite Bands at 30°C , -60°C , and -150°C	63
7	List of Infrared Absorption Bands of Brucite	83
8	Separation of Brucite Bands from 3649 cm^{-1}	91

LIST OF ILLUSTRATIONS

Figure Number		
1	Brucite Crystal Structure	7
2	Brucite Spectrum, 1μ - 15μ (from Coblentz)	12
3	Brucite Spectrum, 2μ - 3μ (from Plyler)	14
4	Brucite Spectrum, 1μ - 2.5μ (from Louisfert)	17
5	Spectra of Brucite Crystal and Powder and Chemically Prepared $Mg(OH)_2$ (from Duval and Lecomte)	20
6	Top and Side Views of Microilluminator	28
7	Top and Front Views of Orientation Cell	31
8	Brucite Spectrum, Incident Beam Parallel to c-axis (NaCl)	43
9	Spectra of Brucite Crystal and Powder (NaCl)	45
10	Spectra of Brucite with c-axis at Various Angles to Incident Beam (NaCl)	47
11	Polarized Spectra of Brucite with c-axis at 45° to Incident Beam (NaCl)	48
12	Spectrum of Chemically Pure $Ca(OH)_2$ (NaCl)	51
13	Spectrum of $Mg(OD)_2$ Powder (NaCl)	53
14	Spectrum of Brucite with Incident Beam Normal to c-axis (NaCl)	56
15	Polarized Spectra of Brucite with Incident Beam Normal to c-axis (NaCl)	58
16	Spectra of Brucite at $30^\circ C$ and $350^\circ C$ (NaCl)	60

Figure
Number

17	Spectra of Brucite at 30°, -60°, -150°C (NaCl)	64
18	Spectra of Exposed Brucite Powder and Chemically Pure MgCO ₃ (NaCl)	67
19	Spectra of Brucite with Incident Beam Parallel and Perpendicular to c-axis (LiF)	69
20	Polarized Spectra of Brucite with Incident Beam Perpendicular to c-axis (LiF)	71
21	Spectra of Brucite (LiF)	73
22	Spectra of Brucite with Incident Beam Parallel and Perpendicular to c-axis (LiF)	75
23	Polarized Spectra of Brucite with Incident Beam Perpendicular to c-axis (LiF)	77
24	Spectra of Brucite with c-axis Parallel to Incident Beam and at 45° and 60° (LiF)	80
25	Alternative Types of Energy Level Diagrams	92
26	Superimposed Mg(OH) ₂ and Mg(OD) ₂ Spectra (LiF)	98
27	Simple Example of Multiple OH Modes	106
28	Suggested Structure of Brucite	108
29	Equivalent Bonding Structures	110

INTRODUCTION

In the course of a study of the infrared spectra of a number of crystalline materials, primarily the micas, it became important to make a detailed investigation of the spectrum of a crystal of known structure containing hydroxyl ions. Furthermore, it was desirable that the crystal structure should be simple, and it was preferable that the OH ions should be oriented in the same direction and be free of hydrogen bonding. The purpose was twofold. First, to decide whether infrared spectral methods could successfully supplement x-ray diffraction work in fixing the hydrogen atom positions in ionic crystals. Second, to study the differences, if any, between the infrared properties of ionized and unionized OH groups.

The search for a crystal satisfying these criteria led to brucite, $\text{Mg}(\text{OH})_2$, whose crystal structure had been deduced from x-ray diffraction work. The structure was reported to be relatively simple with all the hydroxyl ions oriented in the same direction and no hydrogen between them. Moreover, the mineral is readily available, and it is easy to prepare suitable single crystals for infrared transmission spectra. From all points of view, brucite seemed to be the ideal substance on which to begin the

study of the infrared spectra of "free" hydroxyl ions in the crystalline state.

With this knowledge of previous investigations, it was expected that the infrared spectrum of brucite would show a single strong band near 2.75μ which would exhibit complete polarization. It is sufficient to state here that this follows from the unit cell deduced from the positions of the O and Mg atoms and from the proposed orientation of the OH ions. However, the first spectra of brucite that were obtained exhibited an extraordinary complex of absorption bands in the neighborhood of the OH stretching frequency. Some bands were present only for particular orientations of the crystal relative to the direction of the incident light, and many of them displayed a variety of polarization properties. These results were certainly unexpected in view of the previously accepted structure of the brucite crystal.

The question that immediately comes to mind is how many of the bands in this complex are OH stretching fundamentals. If there are more than one, then the previous structure determination with regard to the OH orientations is incorrect. If the OH orientations are different from those proposed, then the unit cell of the brucite crystal must be different from that deduced simply from the oxygen and magnesium positions. Since x-ray techniques cannot locate the hydrogen atoms directly, this appeared to

be an excellent opportunity to apply the sensitive tools of infrared to fix the hydrogen atom positions in an ionic crystal. The spectrum of deuterated brucite should be of help in assigning those bands which are OH frequencies, and spectra obtained with various crystal orientations and with polarized radiation should yield a great deal of information about the OH directions in the crystal.

The study presented here is principally an attempt to decide upon the following questions.

1. Are all the hydroxyl ions in brucite aligned in the same direction as previously proposed?
2. Is the unit cell of brucite as given by x-rays correct?
3. Are the OH vibrations free of hydrogen bonding?

The deductions made from x-ray data would give affirmative answers to these three questions. However, infrared evidence as given here favors negative answers to all three questions. Suggestions are made for an alternative structure for brucite, satisfying old x-ray and new infrared observations.

All pertinent previous studies on the structure of brucite are reviewed in Chapter 1. The apparatus and experimental techniques used in the work are described in Chapter 2. The experimental results and the important spectra are given in Chapter 3, while Chapter 4 contains a statement of the conclusions reached as a result of this investigation.

CHAPTER 1

REVIEW OF PREVIOUS WORK

1.1 General Properties

Brucite, $\text{Mg}(\text{OH})_2$, is a mineral which occurs most often in metamorphic calcite-brucite rock as an alteration of periclase, MgO . Sometimes it is also found in serpentine, $3\text{MgO} \cdot 2\text{SiO}_2 \cdot 2\text{H}_2\text{O}$ ¹. The mineral was discovered by A. Bruce in 1814 at Hoboken, New Jersey, and its present name was assigned in 1824.

Brucite crystals occur in plates or scaly aggregates and are colorless in thin sections. A fibrous variation, nemalite, has been found which has been shown by x-ray diffraction methods to have the same crystal structure as the more common form. The crystal is uniaxial and is cleaved easily in planes normal to the optic axis. In contrast to the very elastic cleaved sections of mica, those of brucite are soft and brittle. The indices of refraction have been measured by several investigators; the values given by Rogers and Kerr¹ are $n_\omega = 1.566$ for the ordinary ray

The text is divided into Chapters and subdivisions or sections. These are labeled so that the first number gives the Chapter and the second number gives the section in that Chapter, e.g. 2.3 means section 3 in Chapter 2.

and $n_e = 1.585$ for the extraordinary ray. Thus, only moderate birefringence is observed.

The specific gravity of chemically prepared $Mg(OH)_2$ depends upon the method of preparation, but it is always less than that of the natural crystal, given to be in the range 2.38-2.40 in the Handbook of Chemistry and Physics². This divergence in values is noted in other specific gravity determinations and is assumed to arise from differing impurity content. Brucite has a hardness of 2 on Mohs' scale.

It has generally been assumed that brucite is a true hydroxide rather than a hydrate of magnesium oxide, $MgO \cdot H_2O$.

Water cannot be driven from brucite for temperatures below $350^\circ C$ ³. Giaque and Archibald⁴ have studied the specific heat of brucite. They found that the specific heat at constant pressure varies from 0.082 cal/mol deg. at $20^\circ K$ to 19.18 cal/mol deg. at $320^\circ K$. Also, brucite crystals are pyroelectric⁵. Megaw⁶ has studied the expansion coefficients of brucite and other crystals from $0^\circ C$ to $100^\circ C$ by x-ray methods. The values found for brucite were $4.47 \pm 0.20 \times 10^{-5}$ along a direction normal to the cleavage plane and $1.10 \pm 0.15 \times 10^{-5}$ for a direction parallel to the cleavage plane.

The ease of cleavage of the brucite crystal means that quite suitable thin sections are easily available for infrared investigation. It is also possible to cut and grind crystal plates with faces perpendicular to the cleavage

plane. The method of preparing such samples will be discussed in detail in a later section.

1.2 X-ray Diffraction Studies

The crystal structure of brucite was first determined by G. Aminoff⁷ in 1919 using x-ray methods. The crystal has been shown to be hexagonal of the CdI_2 type having the symmetries of a D_{3d}^3 space group. That is, the unique c-axis of the crystal is directed normal to the cleavage planes, and the three equivalent a-axes intersect at 60° angles in a plane normal to the c-axis. The plane in which the three a-axes lie is designated as the (0001) plane, where the numbers represent Miller indices. A Miller index is the reciprocal of the intercept of a plane on an axis in terms of the unit length along that axis. The first three indices indicate the intercepts along the three a-axes, and the last index gives the intercept along the c-axis. Thus, the (0001) plane is parallel to the plane containing the three a-axes (intercepts at infinity) and cuts the c-axis at a distance c from the origin.

Diagrammatic representations of the crystal structure are given in Fig. 1, and these aid in picturing the relative positions of the various atoms and ions. The Mg ions lie in the (0001) planes. When viewed along the c-axis, Fig. 1(a), one sees that each Mg ion lies in the center of six hydroxyl ions which in turn are situated at the corners of a hexagon. The hydroxyl ions are in planes

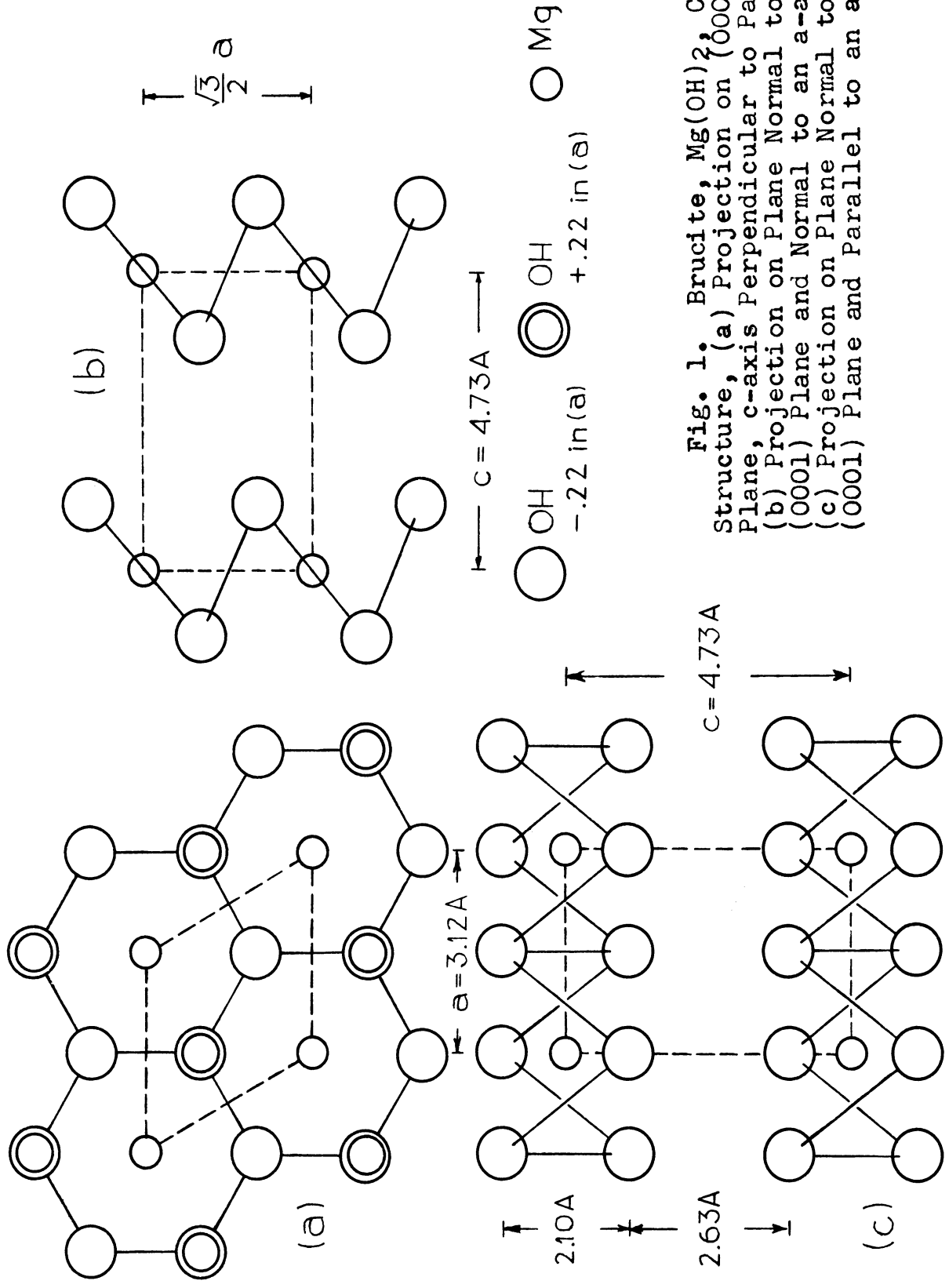


Fig. 1. Brucite, $Mg(OH)_2$, Crystal Structure, (a) Projection on (0001) Plane, c-axis Perpendicular to Page, (b) Projection on Plane Normal to (0001) Plane and Normal to an a-axis, (c) Projection on Plane Normal to (0001) Plane and Parallel to an a-axis.

which are parallel to the (0001) plane and at distances $0.22c$ and $-0.22c$ from it. Thus, the hydroxyls pictured in Fig. 1(a) are alternately above and below the plane of the Mg ions. The Mg and OH ions situated on these three planes constitute a layer in the layer lattice structure of brucite. The neighboring layer is formed about a plane of Mg ions which is at a distance c from the first plane of Mg's. Each ion in the succeeding layers is directly above the corresponding ion in its neighboring layer, so that the layers are not displaced with respect to each other. The hydroxyl ions of adjacent layers form hexagonal close packing, and the cleavage occurs between these layers, i.e. at alternate (0002) planes. On one side of each hydroxyl, the nearest neighbors are three Mg ions from its own layer, while three OH ions of the next layer are nearest on the other side.

Aminoff⁸ measured the axes to be $a = 3.13A$ and $c = 4.75A$. Later x-ray studies gave varying values for these dimensions. These are reviewed in Table 1.

The dimensions of the unit cell given in Fig. 1 are those of Trendelenburg and Wieland which are given in the Strukturbericht. Using these values, other important distances may be calculated from the geometry of the crystal. The closest hydroxyls in neighboring layers lie $3.22A$ apart, and the shortest OH-OH distance within a layer is $2.77A$. The OH-OH distances in a plane of hydroxyls is $3.12A$.

Table 1
UNIT CELL DIMENSIONS OF BRUCITE

<u>a</u>	<u>c</u>	<u>Reference</u>
3.13 A	4.75 A	Aminoff ⁸
3.114	4.735	Levi and Ferrari ⁹
3.117	4.74	Natti and Passerini ¹⁰
3.15	4.78	Bury and Davies ¹¹
3.142	4.758 ± .003	Megaw ⁶
3.12	4.73	Trendelenburg and Wieland ¹²
3.125	4.752 ± .005	Garrido ¹³

Thus, the layers of brucite are composed of Mg ions centered in puckered hexagons of OH ions. The layers are assumed to be held together by weak secondary forces (e.g. van der Waals forces) existing between the planes of hydroxyl ions of neighboring layers. These forces must be relatively weak compared to the other forces in the crystal, since perfect cleavage is easily accomplished between the layers.

Bernal and Megaw¹⁴ performed an extensive x-ray study of various crystals containing hydroxyl ions. Among the substances studied were $\text{Mg}(\text{OH})_2$, $\text{Ca}(\text{OH})_2$, $\text{Co}(\text{OH})_2$, $\text{Ni}(\text{OH})_2$, $\text{Fe}(\text{OH})_2$, and $\text{Cd}(\text{OH})_2$, all of which possess the same crystal structure as determined by x-ray methods. The purpose of their investigation was to elucidate the role of

hydrogen in intermolecular forces, primarily those forces which occur between hydroxyl ions. From the fact that relatively large distances were involved between layers of brucite, and since the OH ions packed together in hexagonal close packing, Bernal and Megaw concluded that the hydroxyl ions of neighboring layers did not influence each other through hydrogen bonding. With the hydrogen free of any influence due to nearby hydroxyl ions, they felt that it would be situated as far from the Mg ions as possible, so that the O-H directions would be normal to the (0001) plane of the Mg ions, i.e. parallel to the c-axis.

A fibrous form of the natural crystal is also found, but it has the same crystal structure as the more common plates¹³. The x-ray data also show that natural brucite and chemically prepared $Mg(OH)_2$ crystals possess the same crystal structure.

1.3 Infrared Studies

When the study of materials through their infrared spectra was still in its infancy (as it may yet be), Coblentz¹⁵ obtained the spectra of a vast array of substances. He used a rock salt prism to cover the region from 1μ to 15μ , and as was necessary in that era, a laborious point by point plot was made of the percent transmission as a function of the wave length. In spite of crude techniques, Coblentz made a considerable contribution to the understanding of the significance of infrared

absorption of molecules and crystals. Part of this voluminous investigation was designed to differentiate between water of crystallization and water of constitution by spectral methods. Coblentz showed that water of crystallization possesses all the spectral characteristics of free water, displaying absorption bands at 1.5μ , 2μ , 3μ , 4.75μ , and 6μ with their relative intensities just as they are observed in the water spectrum.

While Coblentz was able to differentiate between waters of crystallization and constitution, and while he had correlated absorption bands of many substances with the presence of H_2O and OH groups and ions, the spectrum of brucite was somewhat of an enigma for him. His earlier published spectra showed only a strong absorption maximum at roughly 2.5μ in the 2μ to 3.5μ region.¹⁶ This gave him some concern, since he had expected to find a band near 3μ , which he felt was characteristic of all OH groups and ions. By increasing the resolution of his instrument and using a thinner sample, he was finally able to resolve three bands at 2.5μ , 2.7μ and 3μ . However, his curve showed only ten points from 2μ to 3μ , and it is difficult to know that all absorption maxima were accounted for. The band that Coblentz listed as being at 3μ appears to be closer to 2.9μ in his curve (see Fig. 2), but he was determined to show that $Mg(OH)_2$ had a 3μ band as he had shown existed for all the hydroxyl groups and ions he had studied.

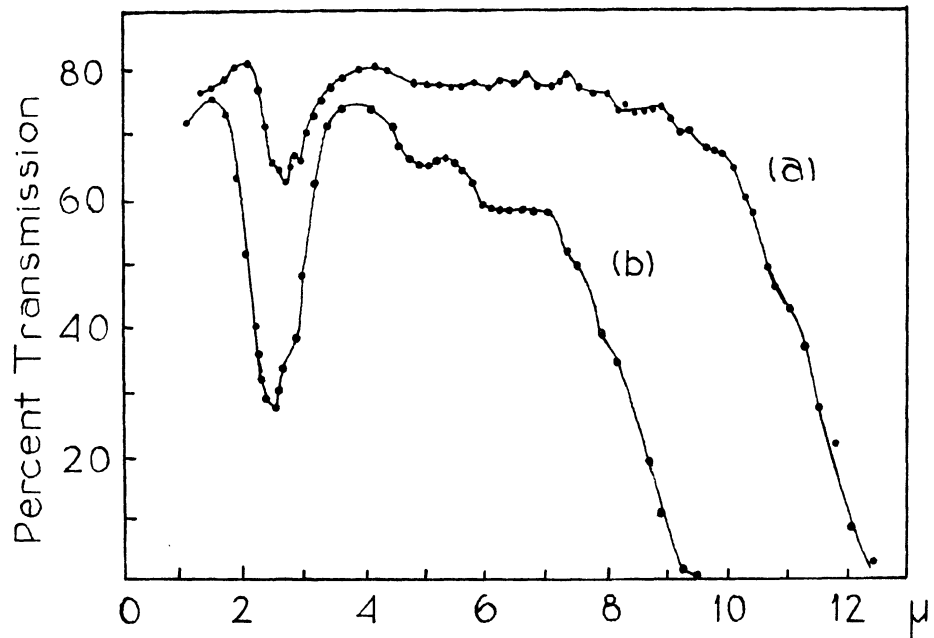


Fig. 2. Spectrum of Brucite, with Incident Beam Parallel to the c-axis (from Coblenz¹⁵).

With reference to this region of the brucite spectrum, Coblenz concludes, "Of course, . . . , by straining matters one might have concluded that the band at 2.5μ , which is evidently complex, contains the 3μ band."

Coblenz was so perturbed by the lack of what he considered an OH band that for a while he proposed that the hydroxyl in $\text{Mg}(\text{OH})_2$ was "inactive."

For the remainder of the 1μ to 15μ range for brucite, Coblenz reported "depressions" in the curve at 5μ , 7μ , 7.7μ , 8.2μ , 9.7μ and complete opacity beyond 12μ for a sample thickness of 0.05 mm.

About twenty years after Coblenz's work, Plyler¹⁷ published a spectrum of brucite in the 2μ to 4μ interval obtained with a rock salt prism (see Fig. 3). Plyler also found the principal absorption maximum to be near 2.48μ . In addition, he observed several shoulders on the short wave length side of this strong band. These were found to be situated at 2.40μ , 2.30μ , and 2.14μ . He also found a slight inflection in his curve at 2.20μ , but he stated that it was probably due to experimental errors. For reasons other than a structural analysis, Plyler was primarily interested in the short wave length side of 2.5μ , and hence he made readings at 0.02μ intervals from 2μ to 2.6μ but only at 0.05μ spacings beyond 2.6μ . None the less, his curve shows as much, if not more, broadening on the long wave length side of 2.48μ , and there is evidence that further absorption maxima and structure may be present from

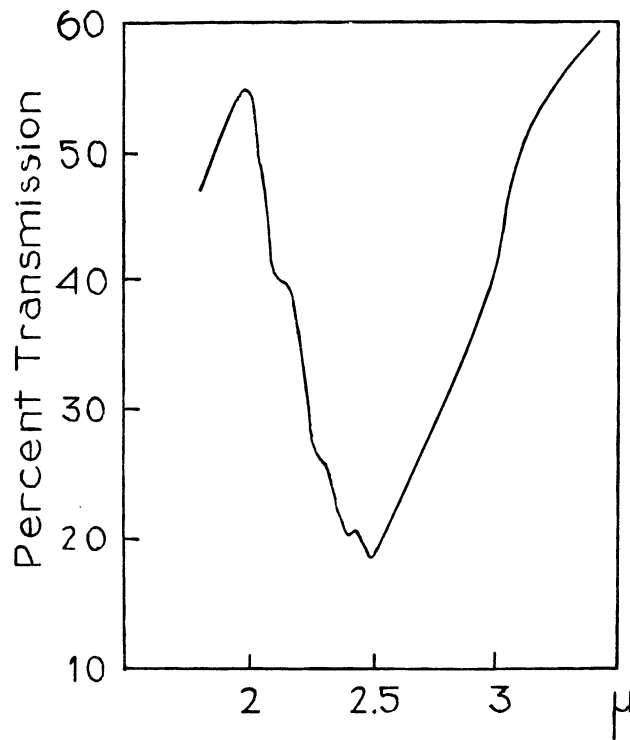


Fig. 3. Spectrum of Brucite,
Incident Beam Parallel to the c-axis
(from Plyler¹⁷).

2.5 μ to approximately 3.1 μ . Plyler also found a band at roughly 1.3 μ , but he did not give a diagram, since, "The true shape of this band could not be obtained because of small rough places on the surface. This causes a greater percent of diffuse reflection for short wave lengths than for long ones."

No further infrared spectra work was published on brucite until 1940 when Yeou Ta¹⁸ reported on the overtone region. Since it had been suggested that the symmetry of the brucite crystal as determined by x-ray analysis might require that the O-H directions be oriented parallel to the c-axis (see 1.2), Yeou Ta investigated the region of the OH stretching overtone. Following the techniques that he had employed previously on the iodoform crystal¹⁹, a brucite crystal plate (0.5 mm. thick) with its faces parallel to the cleavage plane was prepared. When this sample was inclined at an angle of 40° to the incident beam, an absorption band was observed near 7142 cm⁻¹ (approximately 1.4 μ). As the angle between the c-axis (perpendicular to the cleavage plane) and the incident beam was decreased, the intensity of this band diminished. When the c-axis of the crystal was oriented parallel to the beam, i.e. with the cleavage plane normal to the light path, this band was missing entirely from the spectrum. When polarized incident radiation was used, it was noted that this band appeared only when there was a component of the electric vector of the light which was parallel to the c-axis of the crystal.

Unfortunately, none of these curves were given along with the work as presented.

The band at 1.4μ was interpreted as the first overtone of the OH stretching frequency. Thus, the conclusion was made that the O-H directions in brucite were parallel to the c-axis of the crystal. Furthermore, he concluded that the OH vibration was unperturbed by hydrogen bonds, since the absorption band was at a higher frequency than that associated with hydrogen bonds. Yeou Ta stated that these same conclusions could be extended to cover all crystalline hydroxides having the same structure as brucite. These results explain some of Coblentz's confusion. The strong, free OH absorption band near 2.8μ was not present in his spectra of brucite by virtue of the orientation of the crystal with respect to the incident beam of his spectrometer, that is the cleavage plane perpendicular to the light path.

Louisfert²⁰ confirmed the results of Yeou Ta using a flint glass prism to scan the region from 1μ to 2.5μ . In addition to the first overtone of the OH stretching frequency near 1.4μ , bands were reported at three other positions (see Fig. 4). For a brucite crystal cut perpendicular to the c-axis (parallel to the cleavage plane), bands appeared at 2.14μ , 2.32μ , and 2.46μ . For a specimen cut parallel to the c-axis, absorption maxima were found at 1.3982μ , 2.16μ , and 2.32μ . That is, the 1.3982μ band was missing when the incident beam was parallel to the c-axis and present

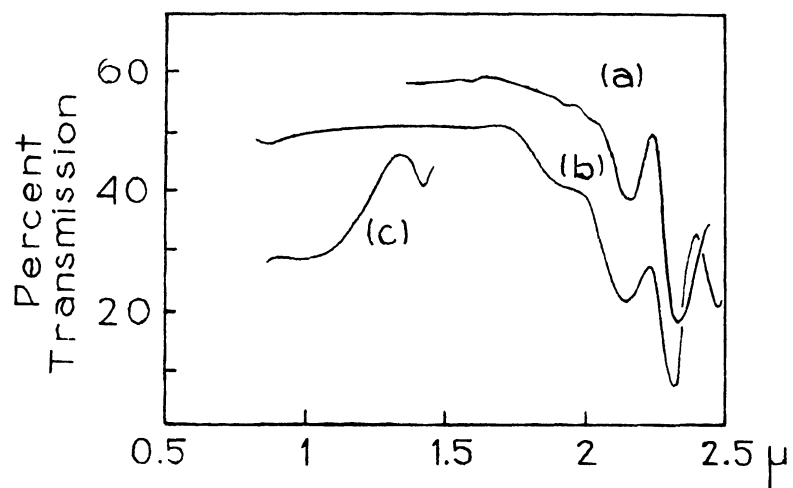


Fig. 4. Spectra of Brucite Crystal Plates, (a) Cut with Faces Parallel to c-axis, 0.20 mm Thick, (b) Cut with Faces Perpendicular to c-axis, 0.37 mm Thick, (c) Cut with Faces Parallel to c-axis, 0.53 mm Thick (from Louisfert²⁰).

when the beam was normal to the c-axis. The opposite effect was noted for the 2.46μ band, which appeared when the c-axis was parallel to the incident beam. The other two bands were present for both orientations, although a shift in position occurred for one, 2.14μ to 2.16μ . Assignments were made for these bands, and they are given below in Table 2.

Table 2
 ASSIGNMENTS FOR BRUCITE BANDS
 (From Louisfert²⁰)

Plates Normal to c-axis	-	2.14μ	2.32μ	2.46μ
Plates Parallel to c-axis	1.3982μ	2.16μ	2.32μ	-
Assignments	$2\nu_{OH}$	$\nu_{OH} + 2\nu_C$	$\nu_{OH} + 2\nu_R$	$\nu_{OH} + \nu_R$

These assignments are somewhat vague, however. By ν_{OH} was meant the OH stretching frequency. The only mention in the text of the paper of ν_R was as a constrained rotation frequency of liquid water (which was listed as being at 19.5μ or 590 cm^{-1} , actually 19.5μ gives approximately 512 cm^{-1}), and no mention of ν_C was made at all. From Table 2, approximate values of ν_R can be found in three different ways, if ν_{OH} is at 2.8μ , i.e. half the overtone frequency. We have that

$$\nu_{\text{OH}} + 2\nu_{\text{R}} = 4310 \text{ cm}^{-1}$$

$$\nu_{\text{OH}} + \nu_{\text{R}} = 4070 \text{ cm}^{-1}$$

$$\nu_{\text{OH}} = 3575 \text{ cm}^{-1}$$

From these, we get

$$\nu_{\text{R}} \approx 1/2(4310-3575) = 368 \text{ cm}^{-1}$$

or

$$\nu_{\text{R}} \approx (4070-3575) = 495 \text{ cm}^{-1}$$

or

$$\nu_{\text{R}} \approx (4310-4070) = 240 \text{ cm}^{-1}$$

In a similar way, one can find ν_{C} .

$$\nu_{\text{C}} \approx 1/2(4650-3575) = 538 \text{ cm}^{-1}$$

No mention was made of these frequencies in the paper. And although such a thing is surely possible, no discussion was made of the fact that the bands assigned as $\nu_{\text{OH}} + 2\nu_{\text{R}}$ and $\nu_{\text{OH}} + \nu_{\text{R}}$ have such different dichroic properties (see Fig. 4 and Table 2).

Duval and Lecomte^{21,22} reported on the spectrum of brucite in the 5μ to 13μ region using a rock salt prism. They presented the spectra of chemically prepared $\text{Mg}(\text{OH})_2$, finely pulverized brucite, and crystalline brucite (see Fig. 5). For the spectrum of the crystal, the cleavage plane was normal to the light path. A band was located which was said to be at 1538 cm^{-1} or 6.5μ (although it appears to be somewhat different in different curves) in the spectra of the chemically prepared $\text{Mg}(\text{OH})_2$ and the powdered brucite. The absorption maximum did not appear in the spectrum of the brucite crystal. (The small dip

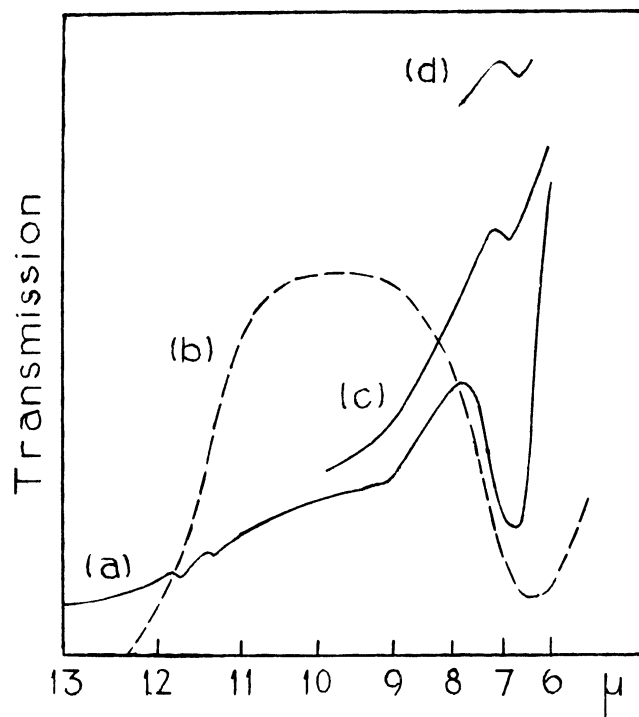


Fig. 5. Spectra of (a) Chemically Prepared $\text{Mg}(\text{OH})_2$, (b) Finely Pulverized Brucite, (c) Brucite Plate 0.7 mm. Thick, and (d) Atmospheric Water Vapor (from Duval and Lecomte²²).

in the crystal spectrum was attributed to atmospheric water vapor.) Duval and Lecomte assigned this absorption band as an OH deformation fundamental frequency, which offers no component of dipole moment change to the incident electric vector when the crystal is oriented with its cleavage plane normal to the incident beam. However, when a powder is used, the OH ions present a random orientation to the incident light, and the band near 6.5μ appears.

Some serious objections may be raised to the conclusions made by Duval and Lecomte. They made reference to Yeou Ta's work, and they concurred with his conclusions that the O-H directions were parallel to the c-axis and that the OH vibration was free. However, if the O-H directions are parallel to the c-axis, they cannot have a deformation fundamental that results in a dipole moment change which is also parallel to the c-axis. In addition, if no hydrogen bonding occurs, then the OH deformation frequency should be at wave lengths longer than 6.5μ .

The powdered specimen was prepared by grinding the crystal and passing the resultant powder through a fine silk screen (No. 230) onto a rock salt plate. The powder was then covered with another rock salt plate to hold it in place. Duval and Lecomte stated that they made no effort to keep either the chemically prepared $Mg(OH)_2$ or the powdered brucite from the atmosphere. However, it is known that the CO_2 in the atmosphere can combine with $Mg(OH)_2$ to form $MgCO_3$ ²³, and experience in the present

study shows that this is especially true with finely powdered samples. The MgCO_3 spectrum exhibits strong absorption in the region 6.5μ to 7μ and two weaker bands at roughly 11.25μ and 11.65μ . These features are present in the powder spectra of Duval and Lecomte. Work in the present study shows that when powdered samples are kept free from the atmosphere, no absorption band is observed in the 6.5μ - 7μ interval for sample thicknesses comparable to those reported by Duval and Lecomte (They used thicknesses "of microns or tens of microns."). Thus, it appears that the powder samples used by Duval and Lecomte had to some degree been converted to carbonate.

Keller and Pickett²⁴ presented a spectrum of brucite along with those of many other minerals. The samples were milled in nujol, and the spectra were obtained with a Beckman Model IR-2 spectrometer equipped with a rock salt prism. The 2μ to 15μ region was covered. Unfortunately, the spectra are obscured and dominated by the absorption bands of nujol, and the brucite bands are shallow and diffuse. None the less, from the fact that the spectrum shows an absorption maximum in the 2.5μ to 2.6μ region, Keller and Pickett concluded that brucite contains free OH groups. No other characteristics of the brucite spectrum were reported, except that there was strong absorption beyond 8μ .

Hasche²⁵ measured the reflectivity of $\text{Mg}(\text{OH})_2$ in the near infrared region, and the results are given in Table 3. No mention was made of the form of the $\text{Mg}(\text{OH})_2$ sample used,

but it is likely that it was a brucite plate.

Table 3
REFLECTIVITY OF BRUCITE
(From Hasche²⁵)

Wave Length in Microns	1.0	1.5	2.0	2.5	3.0	3.5	4.0	4.5	5.0
% Reflected	34.8	25.5	15.4	9.7	3.3	0	0	0	0

CHAPTER 2

APPARATUS AND EXPERIMENTAL PROCEDURES

2.1 Infrared Spectrometers

A Perkin-Elmer Model 21 double-beam infrared recording spectrophotometer was used to cover the 1μ to 15μ region. This instrument was equipped with a rock salt prism. The details of the spectrometer were described by White and Liston²⁶, and it suffices here to report that the spectrum is recorded on a chart indicating percent transmission versus wave length in microns, both on linear scales. The instrument's performance was stable and reproducible within any measurable error. However, the compensation of atmospheric absorption was only fair, the 4.3μ CO_2 band being present with roughly 3-5% peak absorption. The 6μ water bands were not fully compensated either, but this was less bothersome, since the bands are not as intense as the 4.3μ CO_2 band. Also, the 15μ CO_2 band was not fully compensated.

Since most of the interest was centered on the 2μ to 3.1μ interval, it was necessary to have recourse to higher resolving power than a rock salt prism could deliver over this span. To obtain the increased dispersion, a lithium fluoride prism was used in a double-beam spectrometer

designed and constructed at the University of Michigan by Barker and Boettner²⁷. This instrument, in its present state of development, was not as stable nor as versatile as the Perkin-Elmer Model 21, but it did yield the desired increased resolution. Also, the optical path was much longer than for the Perkin-Elmer commercial instruments. As a consequence, atmospheric water vapor absorption left very little energy near 2.75μ to fall on the thermocouple. In addition, there was an impurity in the LiF prism which resulted in a strong absorption band near 2.8μ . Thus, details of a strong absorption band in this region were obscured. This condition was alleviated somewhat by flushing the monochromator with "extra dry" nitrogen. (Bird Gas Co., Detroit, Mich.)

For the spectral region of 15μ to 33μ , a Perkin-Elmer Model 112 single-beam, double-pass spectrometer with a cesium bromide prism was used. The Walsh²⁸ double-pass principle incorporated in this instrument was especially well adapted to reducing the short wave length scattered radiation when observing the longer wave length spectrum. To reduce the atmospheric absorption, the source housing and the monochromator were flushed with "extra dry" nitrogen. A thin CsBr window was attached to the monochromator entrance. Similar windows were placed on the source housing entrance nearest the globar and on an extension tube that extended nearly the full distance between the source housing and the monochromator. While even the thinnest

(15-20 μ) brucite sample prepared was opaque from 13 μ to 33 μ (longest wave length observed), other work showed that the instrument's performance was completely satisfactory.

2.2 Auxiliary Apparatus

For crystals large enough to intercept the light beam completely at the conventional sample position, the specimens were merely mounted on a sturdy piece of cardboard whose center had been cut out to pass the incident light. This proved to be sufficient for some samples which were cleaved along a cleavage plane, but for the most part such large samples were not available.

A microcell was used for smaller specimens. This cell was of such construction that it could be placed at the first focus in all Perkin-Elmer instruments used. The opening in the cell is approximately 14 mm. by 2.5 mm., and this is somewhat larger than necessary. The microcell is described in Perkin-Elmer catalogues, but those used were made by the Physics Instrument Shop at the University of Michigan.

Whenever it was necessary to obtain the spectrum of a mull in nujol, fluorolube, or hexachlorobutadiene, two NaCl or CsBr plates were used to form a usual liquid cell. It was often unnecessary to separate the plates with a shim, since sufficient absorption occurred with thin layers formed simply by pressing the mull between the plates.

Since most samples were not large enough to intercept

the beam of the University of Michigan spectrometer, it was desirable to bring the beam to a focus at an accessible point along the path. This was accomplished by using a pair of bi-convex KBr lenses placed in the path of parallel light at the conventional sample position. The design of this micro-illuminator is shown in Fig. 6 and is due to D. L. Wood, who also ground the lenses. The first lens brings the parallel light to a focus, and the second lens renders it parallel again. In principle, the two lenses are to be placed in the parallel beam two focal lengths apart. But since the lenses are not identical (focal lengths are approximately 47.5 mm. & 49.0 mm. for visible light), some adjustment must be made until the maximum energy is passed through the system. The image size at this point turned out to be somewhat smaller than the aperture of the microcell. Since the wave length interval scanned, 2μ to 3.2μ , was relatively short, it was not necessary to change the lens distances with wave length. However, if a larger region were to be covered, the variation in focal length with wave length would have to be taken into account. This can be seen from the expression for the focal length of a lens.

$$1/f = (n-1) (1/r_1 - 1/r_2)$$

where r_1 and r_2 are the radii of curvature of the lens, f is its focal length, and n its index of refraction. For a

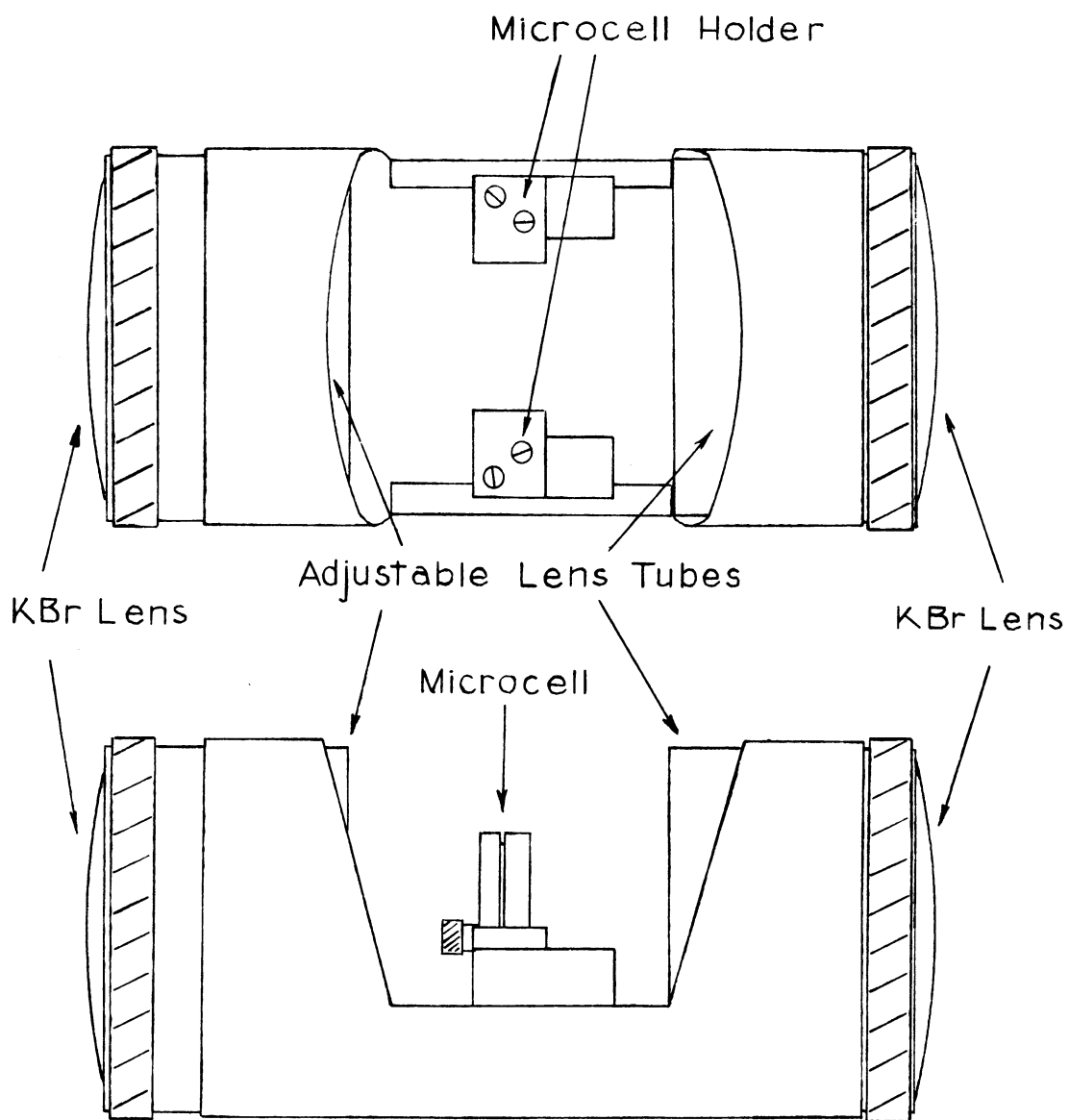


Fig. 6. Top and Side Views of Micrilluminator

bi-convex lens r_1 and r_2 are of opposite sign, so that

$$f = \frac{1}{n-1} \frac{r_1 r_2}{r_1 - r_2} .$$

The index of refraction of KBr for the sodium D line is 1.5581 and at 26μ it is 1.4536. Thus,

$$f_{26} = \frac{0.56}{0.45} f_{\text{vis}} = 1.24 f_{\text{vis}} .$$

For the two lenses used with focal lengths 47.5 mm. and 49.0 mm. in the visible, the focal lengths are 58.9 mm. and 60.8 mm. at 26μ .

The lenses were mounted on the ends of hollow cylinders which can be moved to take account of this variation. Over the 2μ to 3μ region, the focal lengths of these lenses vary only by approximately 0.3 mm.

The heated cell used for spectra at elevated temperature was of conventional design. The cell consisted of a heavy brass holder with shaped NaCl plates enclosing the sample. This cell was then set in a brass cylinder about which was wrapped a layer of asbestos, a heating coil of chromel-D resistance wire, and finally a covering of asbestos. Provision was made for placing an iron-constantin thermocouple at the sample position. Temperatures up to 475°C were recorded. The cold cell used consisted of a brass sample holder constructed to be in contact with a cold reservoir. Provision was made to evacuate the space around the sample holder and reservoir for insulation

purposes. This cell was described in detail by H. B. Kessler²⁹.

For polarized spectra using the Perkin-Elmer double-beam instrument a pair of silver chloride polarizers were used. These were made by Kessler²⁹ from the design of Vallance-Jones³⁰. One polarizer was placed in each beam, and they were set at the same polarizing angle. In this way the polarizing properties of the monochrometer (primarily from reflections at the prism faces) were manifested equally in both beams. A single selenium polarizer was used with the University of Michigan spectrometer, and it was placed immediately before the entrance slit of the monochrometer. The fact that both beams pass through the same polarizer in this instrument is an advantage, since it overcomes the difficulty of matching two of them.

Many spectra were taken of crystal samples oriented at various angles to the direction of the incident beam. For ease and accuracy of these settings, an orientation cell was built. This consists of a brass plate that slides into the cell tracks of any Perkin-Elmer instrument. On the plate is built a pinch holder for the sample, whose angular orientation is read by a pointer on a protractor. The diagram of this cell shown in Fig. 7 is self-explanatory. While this was not built to be a precision instrument, it is felt that the angles were measured to within 2° or 3°.

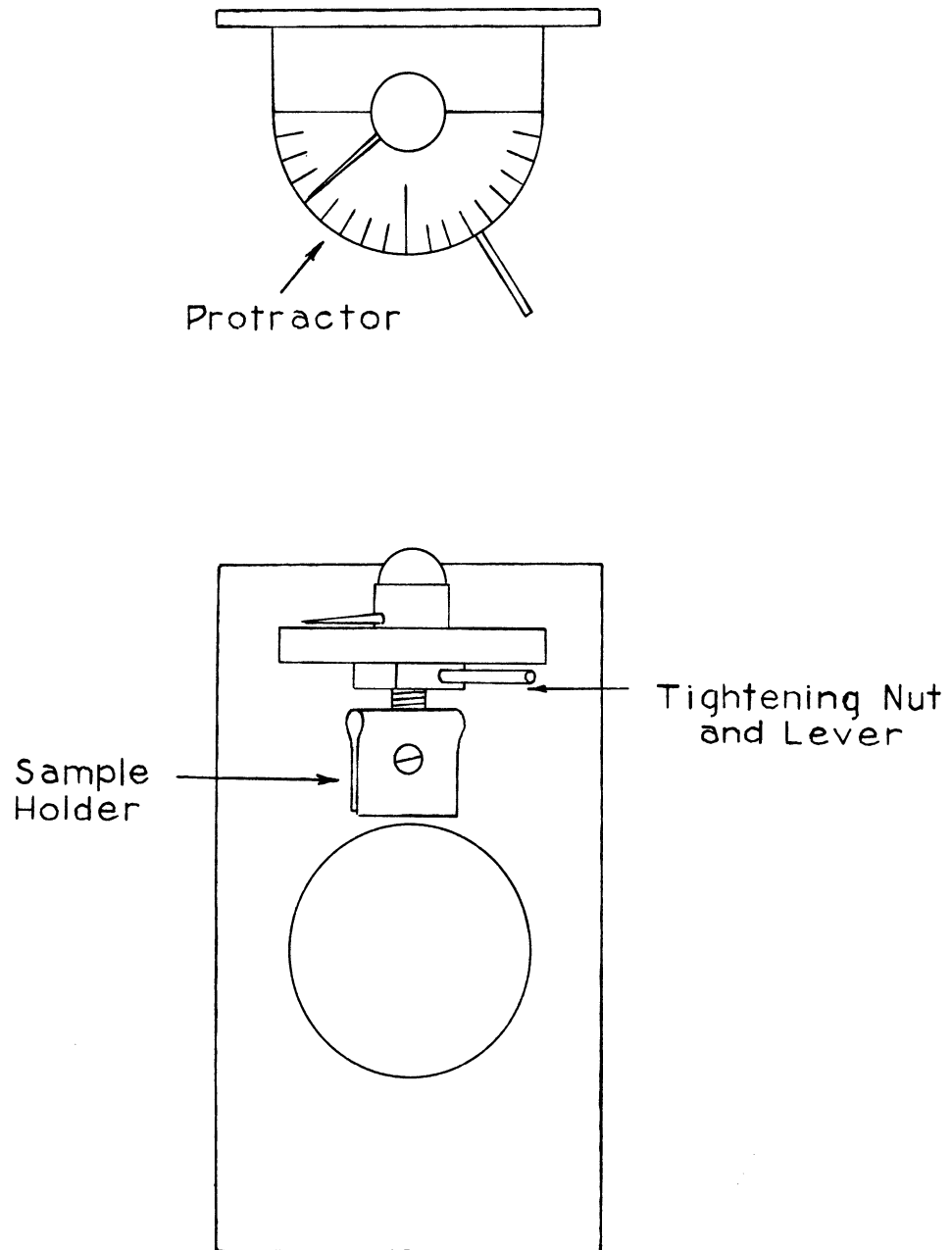


Fig. 7. Top and Front Views of Orientation Cell

2.3 Sample Preparation

As was described in Chapter 1, brucite has a cleavage plane parallel to the (0001) plane of the crystal. The cleavage property of the layered brucite was both an aid and a hindrance to satisfactory sample preparation.

Plates of the crystal with faces parallel to the cleavage plane were easy to prepare. The crystal was cleaved easily with a razor blade or any sharp edge. A razor blade is ideal, since it is thin and does not require the cleaved section to bend very much. Brucite is very brittle, and it will not bend far without breaking. The thinnest cleaved section obtained was approximately 15-20 μ thick. Since brucite is soft (2 on Mohs' scale), it can be cut and shaped to suit most needs. The softness raised a difficulty however, since it allowed samples of perfectly uniform thickness to be cleaved only rarely. This was true because of a tendency of the sharp edge to cut through neighboring layers. However, at times a region of the large natural crystal was found which cleaved perfectly, somewhat in the manner of mica. These regions were only large enough for use with the microcell, i.e. approximately 15 mm. by 5 mm., but they were uniform in thickness, at least to about 3 μ (measured with micrometer that read to 0.1 mil). That is, they were uniform in thickness to about one wave length for spectra from 2 μ to 3 μ .

While the cleavage property of brucite was a help in preparing samples with faces parallel to the cleavage plane, it was a considerable handicap to preparing samples with faces normal to the cleavage plane. Since the forces between layers are relatively weak, only mild agitation is required to break the crystals into fragments. This tendency can be overcome in part in the manner described below.

A natural crystal roughly $1/4$ inch to $1/2$ inch thick in the direction normal to the cleavage plane was cut through with a fine hack saw blade. In this way a relatively smooth surface perpendicular to the cleavage plane was presented. A similar cut was made about $1/2$ cm. from the first. No thinner section could be cut in this way without destroying the sample. One of these nearly parallel faces was ground on an optical grinding wheel until it was relatively smooth and flat. This face was polished on the finest silicon carbide paper, grit number 500. The resulting flat surface was cemented to a flat ground glass plate with a melted mixture of optical pitch and bees wax. The bees wax was used so that the resulting seal would not be too brittle when cooled to room temperature. With the crystal firmly attached to the glass in this way, the exposed face was ground parallel to the polished surface on the fine grinding wheel. This had to be done carefully, for the sample was very brittle. All

grinding had to be done so that the grinding direction was parallel to the cleavage layers, i.e. perpendicular to the weakest forces in the crystal. When the thickness was approximately 300μ , the exposed surface was ground and polished very gently on the silicon-carbide paper. The crystal was removed after the glass plate had been heated to the melting point of the cement. The cement that remained was dissolved with reagent grade acetone.

The above procedure was not entirely satisfactory. The thinnest sections obtained, after many attempts, were approximately 250μ thick. The ideal thickness would have been roughly half this, but these samples were used with considerable success. The polarization spectra showed that crystals prepared in this way were well oriented.

Another method of obtaining thin crystal plates with an edgewise orientation was tried. One face of the crystal was ground and polished as in the first method. The resulting section was embedded in a lucite form using a Buehler metallurgical mounting press. The lucite block was ground down to the unpolished surface of the brucite, and then the brucite and plastic were ground together. The hope was that the plastic would make a firm seal to the crystal and allow thinner samples to be made. The lucite was then to be dissolved from the crystal with acetone. The procedure did not work well for two principal

reasons: (1) the plastic did not adhere to the polished surface as well as had been anticipated, and (2) instead of completely dissolving, the plastic merely softened and diffused into the crystal, making it unsuitable for infrared transmission. However, two samples (approx. 300 μ thick) were obtained by chipping the thin crystals from the solid plastic form. Their spectra confirmed a previous suspicion that several small bands appearing in the sections prepared by the first method were due to residual optical pitch- bees wax mixture which was not fully dissolved. While the embedding procedure was not entirely satisfactory for brucite, this general method of crystal preparation might yield results for other crystals and possibly with other plastics.

At times it was necessary to obtain spectra of powdered samples. These samples were prepared in two ways. If it was important that the powder be kept from atmospheric water vapor or CO₂, then the compound was ground as finely as possible inside a nitrogen flushed dry box (designed and constructed by K. N. Tanner) and mullied in nujol, fluorolube, or hexachlorobutadiene. It was then safe to remove the mull from the dry box, since none of these mulling agents evaporated rapidly enough to expose the powder to the air. The mull was then pressed between two infrared transparent plates. Thus, the spectra could be obtained in those regions in which the mulling agent

was clear. Of those used, hexachlorobutadiene was the most useful, since it exhibited no absorption in the 1μ to 6μ interval. Also, its index of refraction most nearly matched that of brucite, since the powdered brucite was completely invisible when mullied in hexachlorobutadiene. In addition, only slight scattering occurred at the short wave lengths of a spectrum of this mull. Mulls were used for spectra of powdered brucite, and chemically prepared $Mg(OH)_2$, $Mg(OD)_2$, and $Ca(OH)_2$ which combine with the CO_2 of the atmosphere to form carbonates²³.

If on the other hand, the powder could come in contact with the atmosphere, then a second method could be used. The advantage of this second method is that smaller particles can be obtained. The powder was first ground as finely as possible with a mortar and pestle. The powder was placed in a graduated cylinder with isopropyl alcohol. The suspension was shaken and left to settle. The settling time was determined by the size and density of the particles, i.e. by how rapidly they settled in the alcohol. After a suitable time, a top fraction of the suspension was decanted. This fraction, containing the smallest particles, was centrifuged until all the particles were at the bottom of the container. The clear alcohol was poured off except for approximately 1 c.c. The powder was stirred into the remaining alcohol, resulting in a rather dense suspension of fine particles. The suspension was

placed on an infrared transparent plate with an eye dropper. The alcohol was allowed to evaporate, leaving a thin film of powder on the plate. The film adhered sufficiently well to the plate, and the layer could be built up to any desired thickness. The smaller the particles were, the less scattering occurred, especially at short wave lengths (1μ - 4μ). This method of powder sample preparation was suggested by a more involved procedure described by Hunt, Wisherd, and Bonham³¹.

CHAPTER 3

EXPERIMENTAL RESULTS OF PRESENT STUDY

3.1 Introduction

It has been proposed that the O-H bond directions in brucite are oriented normal to the cleavage plane, i.e. parallel to the c-axis (see 1.2 and 1.3). Also, the x-ray diffraction results indicate that the nearest O-O distances between oxygen planes of neighboring layers are too long for hydrogen bonds to occur, so that the OH vibrations should be free of any such interaction. If these proposals are correct, then certain characteristics of the infrared spectrum can be predicted.

(a) Neglecting deformation motions including those due to zero point energy, and assuming that the dipole moment change corresponding to the OH stretching motion is directed along a line joining the O and H atoms, the OH stretching frequency should be observed in the spectrum only when the electric vector of the incident light has a component parallel to the c-axis of the crystal. This follows from the fact that the transition probability, and hence the absorption coefficient, is proportional to the square of the cosine of the angle between the incident electric vector and the direction of dipole moment change.

(b) The OH stretching band should be observed at a relatively high frequency, approximately 3700 cm^{-1} or 2.7μ . This follows if no hydrogen bonding occurs and the vibration is free of any field due to the presence of a nearby negative charge. An experimental correlation has been found^{32,33} between OH frequencies and the O-O distance for a series of crystals. The OH frequency was found to increase with increasing O-O distance, i.e. with a weakening of the hydrogen bond. For O-O distances greater than roughly 2.9 Å, the OH frequency can be said to be free, i.e. the influence of the neighboring O atom is negligible, and no hydrogen bonding occurs. The limiting free frequency lies at approximately 3700 cm^{-1} . X-ray diffraction work indicates that the hydroxyl-hydroxyl distances between neighboring layers in brucite are all approximately 3.2 Å or greater, so that the OH stretching frequency of brucite should be high according to previous proposals.

(c) The OH stretching band should be single, and no fine structure should be observed in the infrared spectrum. The argument for this conclusion is rather simple. It has been shown that the dipole moment change that is relevant to the infrared spectrum is that resulting from the motion of the unit cell of a crystal^{34,35,36}. If all the OH bond directions are parallel to the c-axis as proposed, then the unit cell of the crystal including the hydrogen atom positions is the same as that deduced from

the x-ray data¹⁴ neglecting the hydrogen atoms. Thus, there would be only two OH ions per unit cell. It can be shown from mechanics that the normal modes of two coupled oscillators consist of the in-phase and out-of-phase vibrations of the two oscillators. For the two OH ions oriented parallel to one another, one of these normal modes would result in a net dipole moment change of zero, and hence its corresponding frequency would be infrared inactive. The other normal mode would give a resultant dipole moment change of the unit cell directed parallel to the c-axis, and its corresponding frequency would be infrared active. Therefore, only a single frequency corresponding to the OH vibration should be observed in the infrared spectrum.

Any study of brucite through its infrared spectrum should test these three predictions. The validity of (a) and (b) above can be checked experimentally with little difficulty. If more than one frequency is present, and the separation is sufficient for them to be resolved, then (c) can be invalidated. Of course, it is conceivable that more than one normal mode could be infrared active with the resulting frequencies very near each other, or possibly degenerate, so that the multiplicity could go unobserved. Thus, (c) above can be disproved, but it can never be verified with certainty.

As remarked in 1.3, Yeou Ta's observations in the

region of the OH stretching overtone seemed to substantiate predictions (a) and (b), and while no spectra were given with the paper, mention was made of only a single frequency. On the other hand, both Coblentz and Plyler found indications of absorption in the region of the OH stretching fundamental with the incident electric vector perpendicular to the c-axis of the crystal (see Figs. 2 and 3.) The remainder of this chapter will deal with the experimental results of the present study without detailed reference to previous work.

Those spectra for which (NaCl) is in its description were obtained with the Perkin-Elmer Model 21 double-beam instrument using a rock salt prism. Those marked with (LiF) were taken with the University of Michigan double-beam spectrometer using a lithium fluoride prism. The percent transmission values given on the ordinant of the (NaCl) spectra are often not the true values, since the scale was expanded so that the 100% line was completely off scale. No percent transmission values are given with the (LiF) spectra, but the 0% line is always the bottom of the figure.

3.2 Preliminary Spectra

As a preliminary check on the previous work, spectra were obtained of brucite crystals with the incident beam normal to their cleavage planes, i.e. parallel to their

c-axes. Two of these spectra are given in Fig. 8. The most striking feature of these curves is the resolution of the cluster of relatively sharp bands between 2μ and 3.1μ . While the early work showed absorption in this interval with maximum absorption near 2.5μ (the approximate position of the most intense band in Fig. 8), none of these details were observed. The apparent symmetrical grouping of the four principal bands about the free OH stretching position should also be noted. The five absorption maxima in this region occur at roughly 2.30μ , 2.48μ , 2.65μ , 2.83μ , and 3.07μ . No indication of a band at 2.40μ was found where Plyler reported the presence of a shoulder.

The remainder of the spectrum out to 15μ is generally in agreement with that reported by Coblentz, the most marked feature being a strong absorption at the longer wave lengths. Coblentz found "depressions" at 5μ , 7μ , 7.7μ , 8.2μ , and 9.7μ . Over a large number of spectra of many samples for the present study, shallow bands appeared near 5μ , 6.25μ , 8.3μ and 9.9μ . Weak, but relatively sharp bands were found at roughly 3.35μ , 3.45μ , 7.08μ , and 7.23μ .

The character of the spectrum in the vicinity of the OH stretching fundamental is of the most interest, and much of the present work was concentrated there.

5.3 Spectra of Brucite, Cleaved Sections and Powder

The brucite samples were obtained from the Mineralogy Museum of the University of Michigan, and were originally found

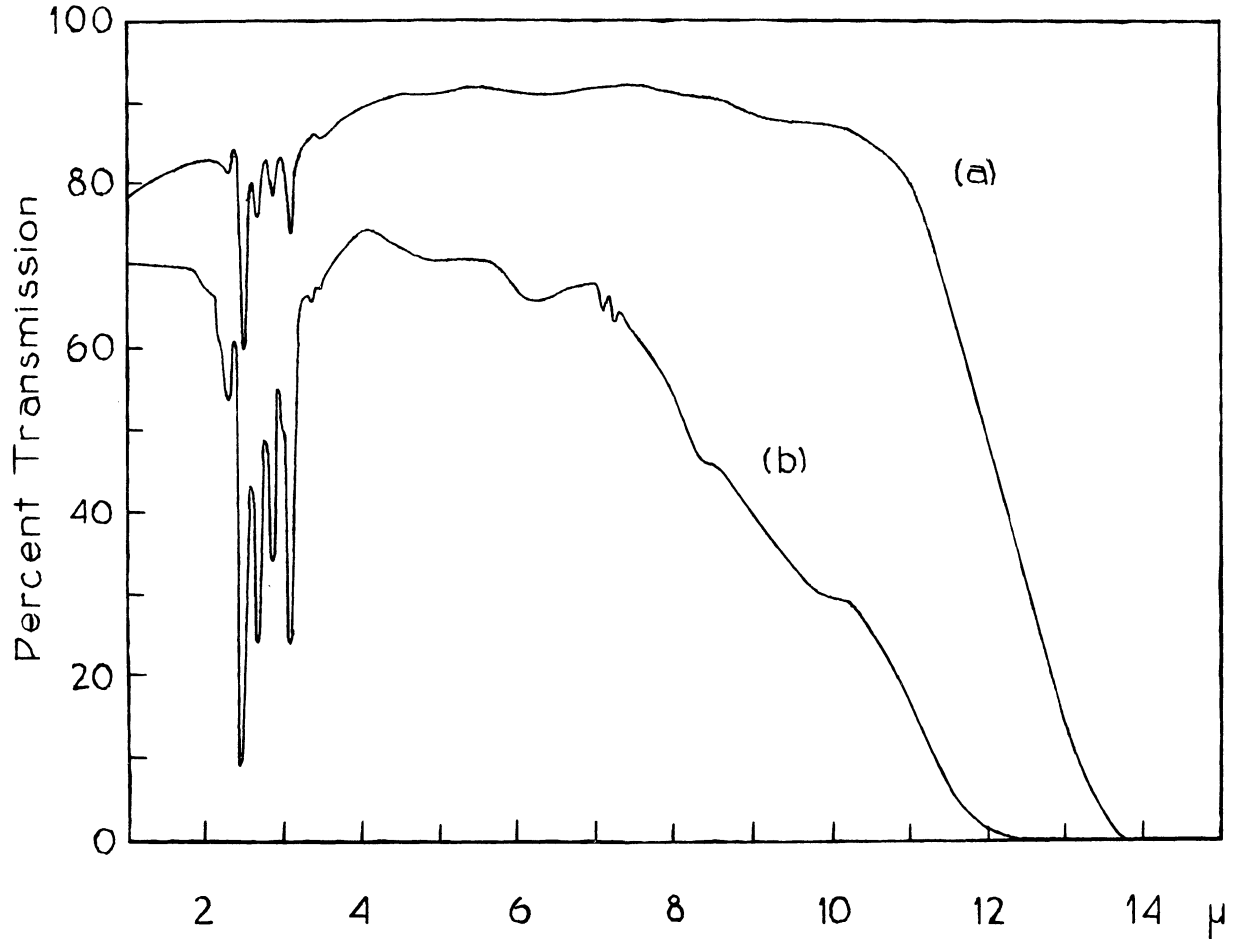


Fig. 8. Spectrum of Brucite with Incident Beam Parallel to the c-axis, (a) 15-20 Microns Thick, (b) Approximately 175 Microns Thick (NaCl).

in Lancaster County, Pennsylvania. From the large natural mass of the mineral, beautiful clear colorless crystals were cleaved and cut. It should be mentioned that in a private communication H. D. Megaw stated that these samples were far better than that which was available for her x-ray diffraction work.

The spectrum over the 2μ to 3.5μ region of a cleaved brucite crystal is shown in Fig. 9(a). The spectrum was obtained with the incident light path normal to the cleavage plane, i.e. parallel to the c-axis of the crystal. A rock salt prism was used for this spectrum, so that the resolving power was relatively low. Nevertheless, the resolution was sufficient to distinguish five distinct maxima, and the presence of so many bands of comparable intensity was somewhat unexpected.

In a powder form, the small crystals present a random orientation to the incident light giving a spectrum which is some kind of average over all possible orientations. To supplement the oriented crystal spectrum in Fig. 9(a), a powdered sample was run in a hexachlorobutadiene mull, and the results are shown in Fig. 9(b). A striking new feature is the strong band that appears near 2.73μ . It is certain that the change in dipole moment corresponding to this band does not present a component to the incident electric vector when the c-axis is parallel to the beam, as for Fig. 9(a).

It is not possible to say what has happened to the

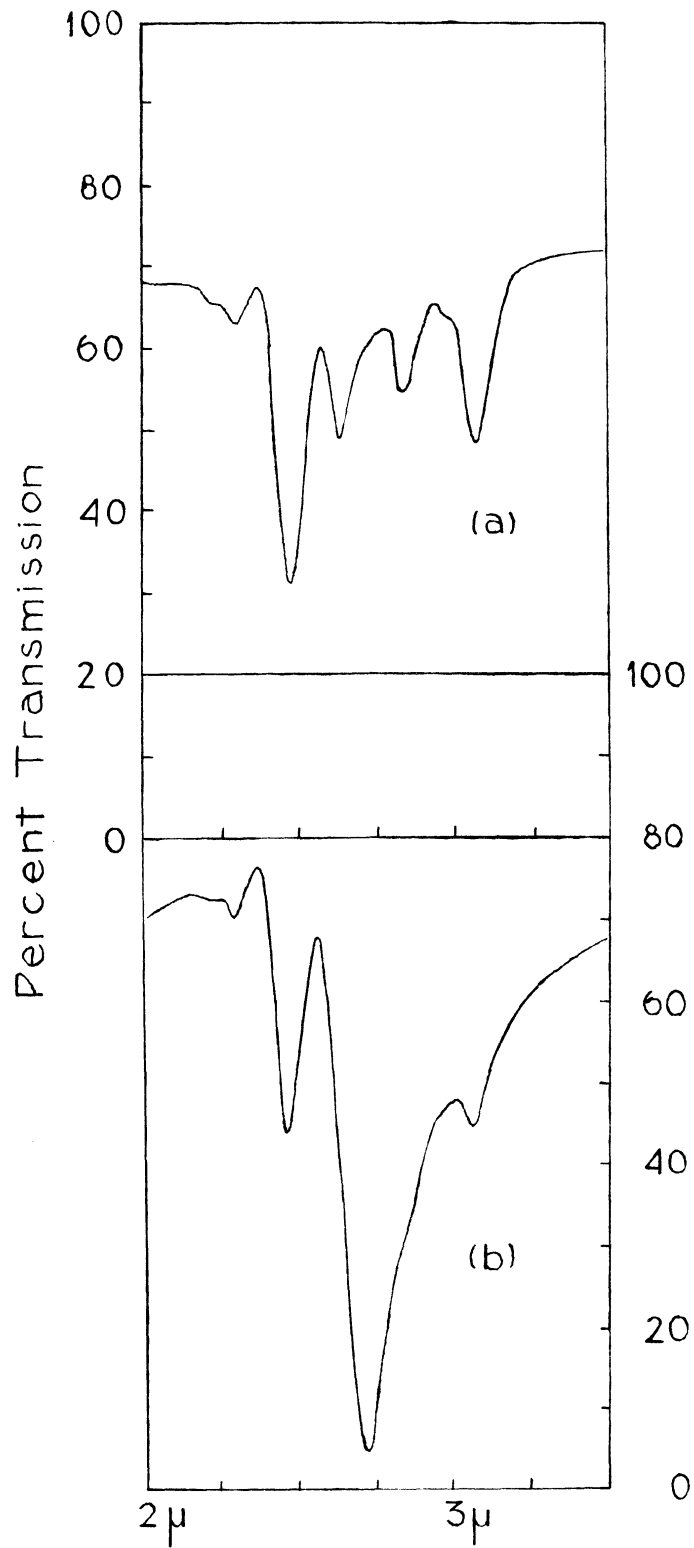


Fig. 9 . Spectra of (a) Brucite Crystal with Incident Beam Parallel to *c*-axis, 140 Microns Thick, (b) Powdered Brucite in Mull (NaCl).

bands near 2.65μ and 2.83μ for the powder spectrum. The manner in which the 2.73μ band develops can be shown by examining the crystal at various angles of inclination between the c-axis of the crystal and the direction of the incident light. The results of such an examination are shown in Fig. 10. The first spectrum is of the crystal in the same orientation as was used for Fig. 9(a), i.e. the c-axis parallel to the incident beam and perpendicular to the electric vector. With inclination of the crystal, the 2.73μ band appears, and its intensity increases with increasing angle, that is with an enlarged component of the electric vector parallel to the c-axis. These spectra also show that the peak intensities of the other bands in this region are approximately constant within experimental error for the various orientations. While the figures are too small to show all details, the band at 2.48μ becomes somewhat broader with increasing angle. It is now possible to understand why the 2.65μ and 2.83μ bands were apparently missing from the powder spectrum in Fig. 9(b). These bands are still present, but they are obscured by the strong 2.73μ absorption. The same results were obtained for rotation of the crystal about any axis parallel to the cleavage plane.

The fact that the dipole moment change responsible for the 2.73μ absorption is directed parallel to the c-axis is also seen from Fig. 11. A cleaved section of brucite is

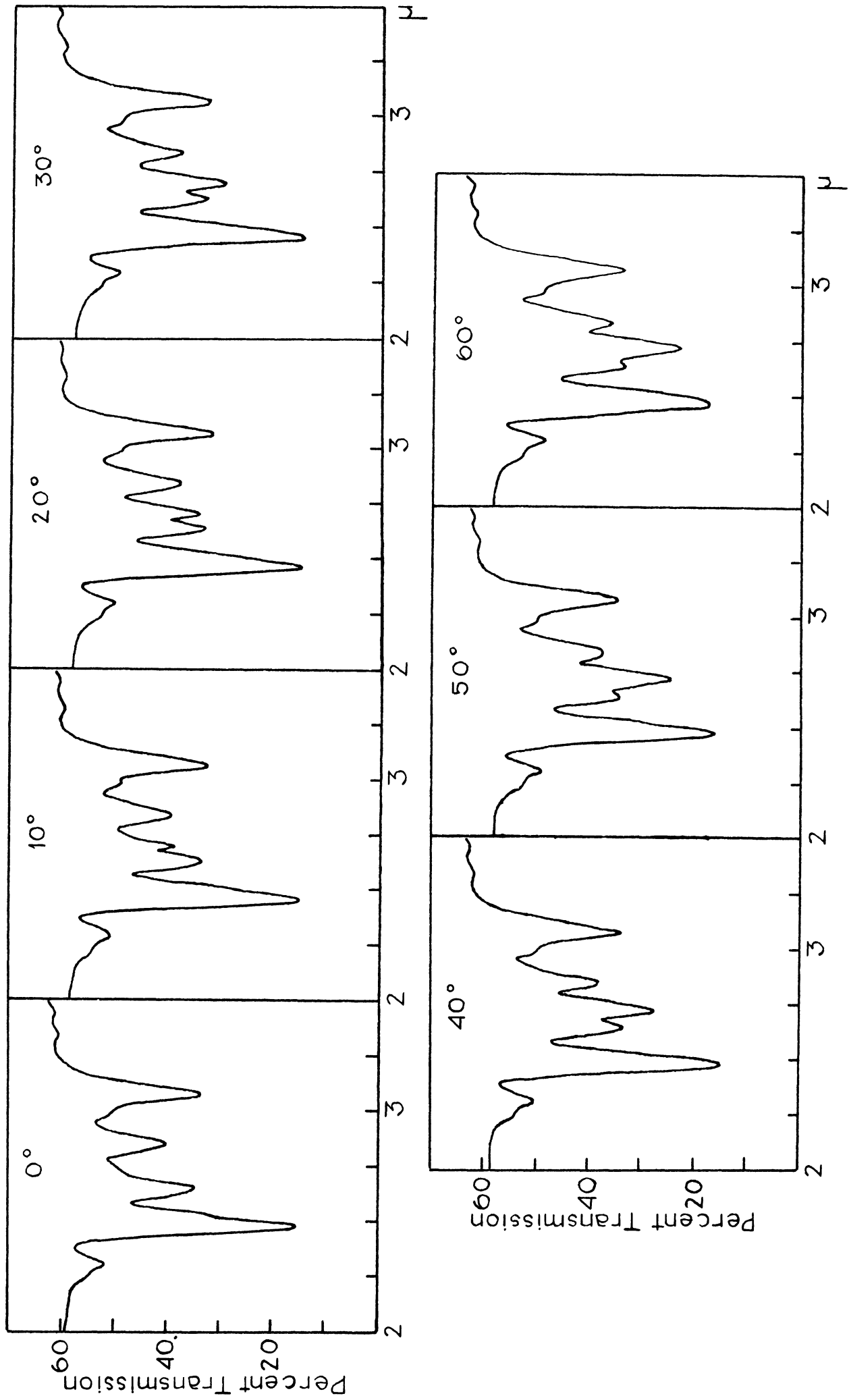


Fig. 10. Spectra of Brucite Crystal 150 Microns Thick with c-axis at Various Angles to the Incident Beam. (NaCl).

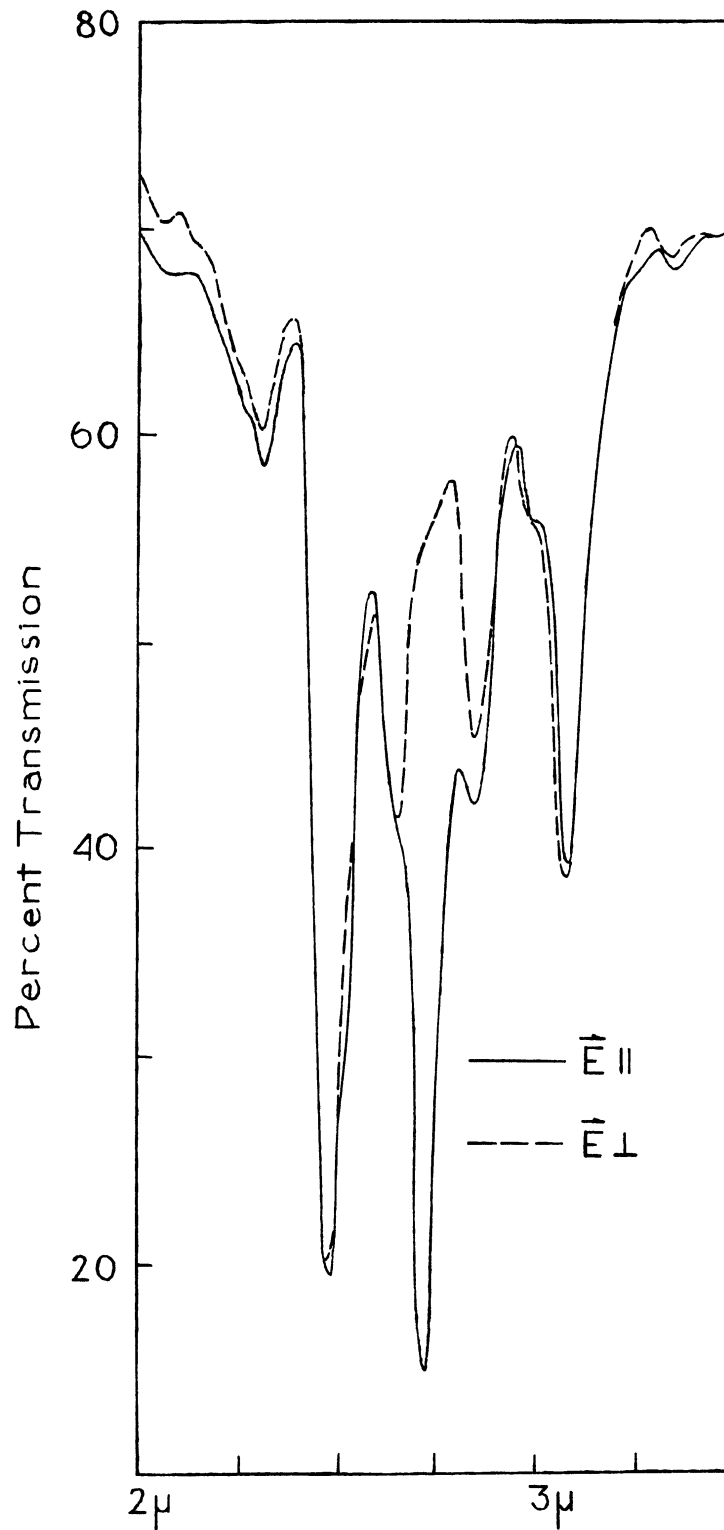


Fig. 11. Polarized Spectra of Brucite Crystal with c-axis at 45° to Incident Beam, Electric Vector Parallel and Perpendicular to Plane Defined by c-axis and Incident Beam (NaCl).

tilted so that the angle between the c-axis and the incident beam is 45° . The polarized spectra show that the 2.73μ band appears only when there is a component of the electric vector which is parallel to the c-axis. This band is completely missing when the electric vector is perpendicular to the c-axis. If the crystal is rotated about any axis parallel to the cleavage plane, the results are unchanged, the 2.73μ band being strongest for the electric vector perpendicular to the rotation axis and missing entirely for the electric vector parallel to this axis.

Other interesting results are brought out by the polarized spectra in Fig. 11, even with the low resolution. Slight shifts in frequency are noticed in the band peaks at 2.48μ and 3.07μ for the two polarization directions.

A band was also observed at roughly 1.37μ , which has exactly the same characteristics as the 2.73μ band (Fig. 14). That is, it appears only when the incident electric vector has a component parallel to the c-axis. Hence, the band at 1.37μ may be safely assigned as the overtone of the 2.73μ absorption.

3.4 Spectra of Chemically Prepared $Mg(OH)_2$ and $Ca(OH)_2$

There might be a question of whether those bands in the 2.0μ and 3.1μ interval, other than the 2.73μ band, are really $Mg(OH)_2$ frequencies. That the entire complex of

absorptions in this region is due to $\text{Mg}(\text{OH})_2$ was shown by two independent methods. (1) A powdered sample of high purity $\text{Mg}(\text{OH})_2$ (supplied by the Michigan Chemical Corp.) gave a spectrum exactly the same as that for powdered brucite (see Fig. 9(b)). This shows that none of these bands are due to the presence of impurities. (2) The spectrum of chemically pure $\text{Ca}(\text{OH})_2$ is given in Fig. 12. Comparison with Fig. 9(b) for $\text{Mg}(\text{OH})_2$ shows the qualitative similarity in the two curves. The $\text{Ca}(\text{OH})_2$ powder used was chemically pure (Mallinkrodt, Analytic Reagent). The $\text{Ca}(\text{OH})_2$ crystal structure, as determined by x-rays, is the same as that of $\text{Mg}(\text{OH})_2$ but with $a = 3.584\text{\AA}$ and $b = 4.896\text{\AA}$.³⁷ Hence, one would expect that the spectra of these two should be qualitatively the same, with a possible shift of position for corresponding bands, since the dimensions of the two are different. In fact, the $\text{Ca}(\text{OH})_2$ band positions have shifted. Those corresponding to the $\text{Mg}(\text{OH})_2$ bands near 2.30μ , 2.46μ , 2.73μ , and 3.07μ appear at approximately 2.38μ , 2.55μ , 2.76μ , and 3.03μ in $\text{Ca}(\text{OH})_2$. The strong central absorption for $\text{Ca}(\text{OH})_2$ is at 2.76μ , and the remainder of the group of bands is compressed closer to this absorption than in the case of $\text{Mg}(\text{OH})_2$.

These spectra of chemically pure substances indicate that the entire group of bands in the 2μ to 3.1μ spectrum of brucite is due to $\text{Mg}(\text{OH})_2$ crystal and not to any impurities in the natural material.

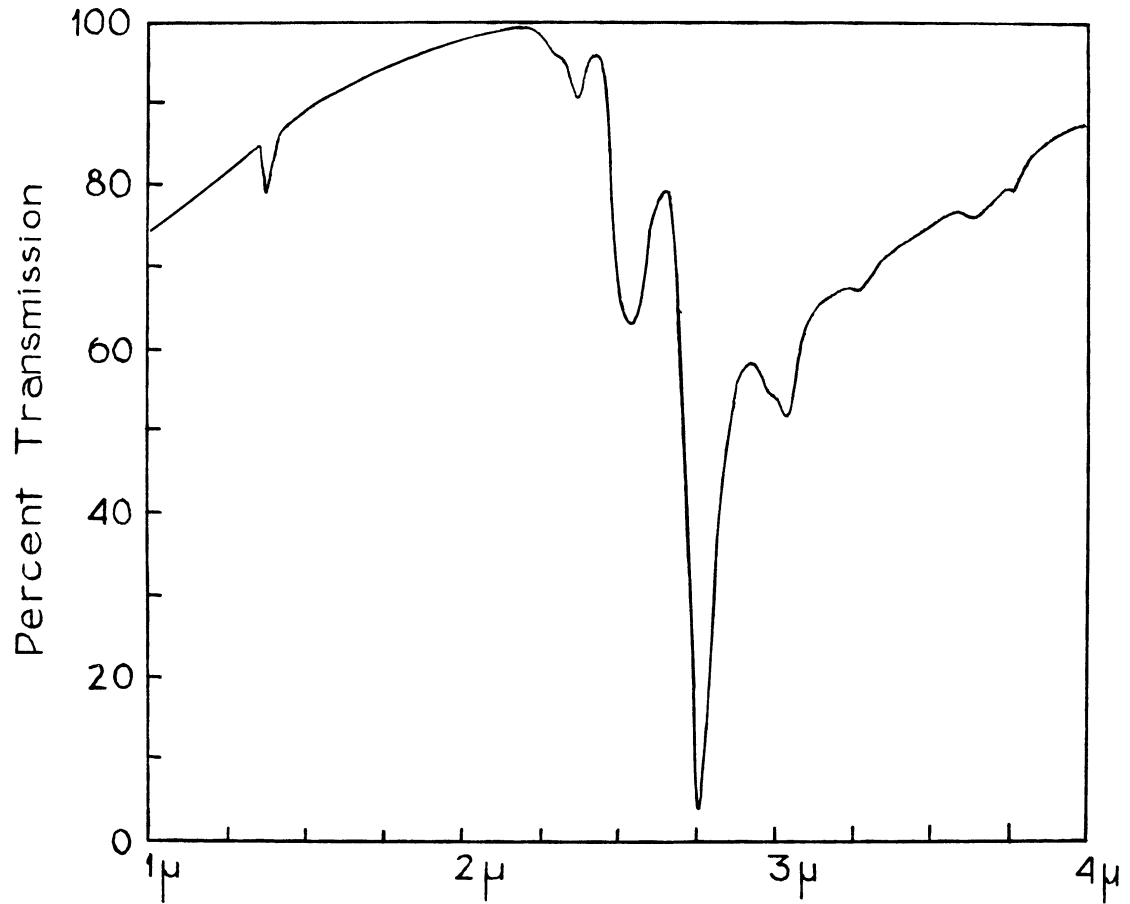
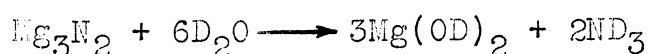


Fig. 12. Spectrum of Chemically Pure $\text{Ca}(\text{OH})_2$ Powder in Hexachlorobutadiene Mull (NaCl).

3.5 Spectrum of Chemically Prepared Mg(OD)₂

The Mg(OD)₂ was supplied by Professor R. W. Parry of the Department of Chemistry at the University of Michigan. The compound was the by-product of a process for making heavy ammonia. The material was prepared through the following chemical reaction.



The resulting compound was said to be 95% deuterated, since the D₂O used was 95% deuterated. The powder spectrum of this specimen of Mg(OD)₂ is shown in Fig. 13. The main absorption bands are now seen to be a group near 3.73μ which has the qualitative characteristics of the 2.73μ group of bands in the undeuterated powder spectrum. In addition, the 2.73μ band is present weakly. This is to be expected, since the compound is not completely deuterated. The incomplete curve in Fig. 13 is for a thicker sample to bring out the weaker bands.

Comparison of the powder spectra of Mg(OH)₂ and Mg(OD)₂ gives an important result. Each absorption band of the Mg(OD)₂ complex whose center is near 3.73μ is at approximately $\sqrt{2}$ times the wave length of the corresponding band for Mg(OH)₂. This result is tabulated in Table 4. The error in the wave lengths given in Table 4 may be as high as ± 0.03μ. The position of the band near 4.35μ for Mg(OD)₂ may be even more in error, since it was difficult

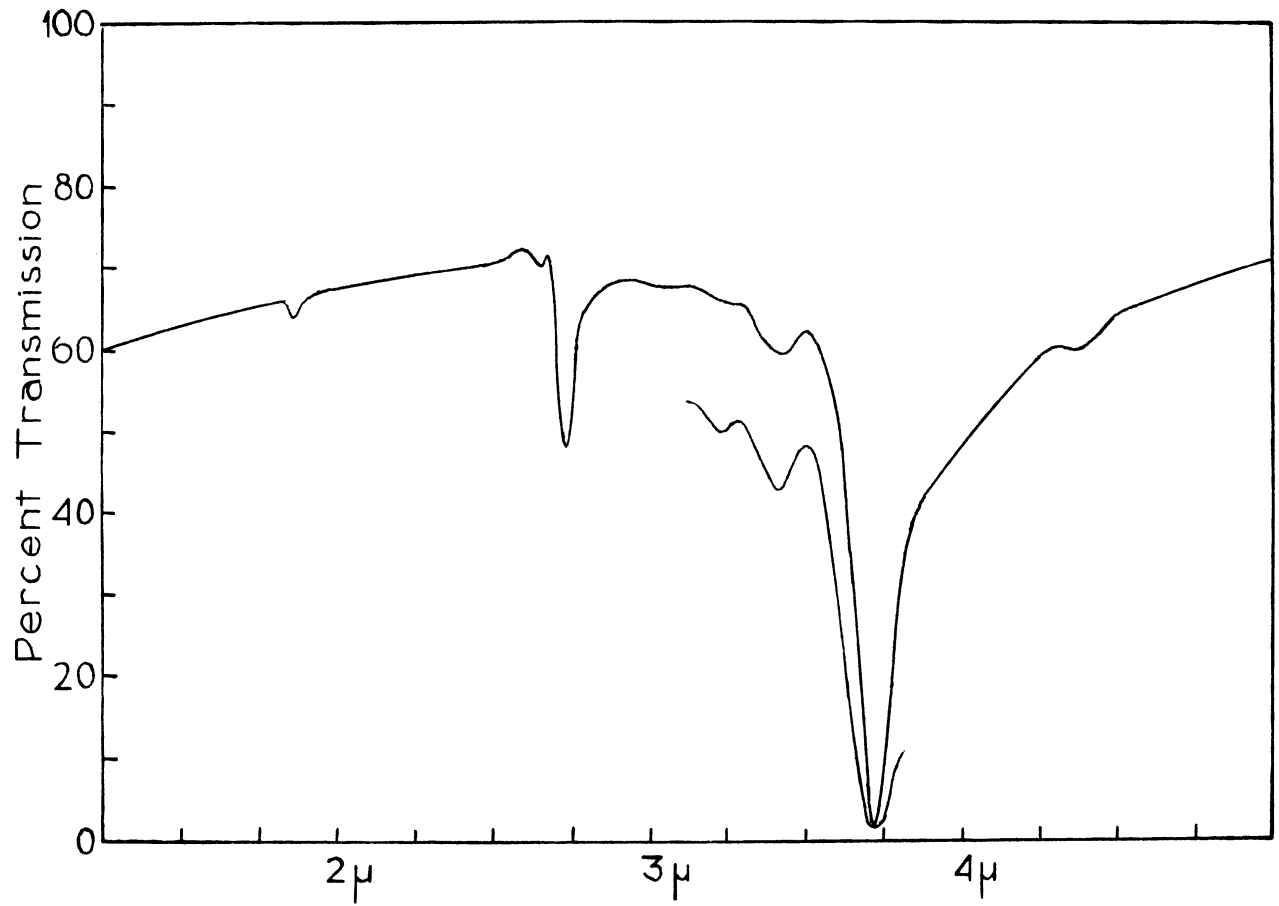


Fig. 13. Spectrum of Chemically Prepared $\text{Mg}(\text{OD})_2$ Powder in Hexachlorobutadiene Mull (NaCl).

to compensate completely for the 4.3μ atmospheric CO_2 band in the Perkin-Elmer Model 21 double-beam instrument. As a consequence, corresponding errors occur in the ratios of the wave lengths given less, the constancy of these r lished.

Table 4
Comparison of $\text{Mg}(\text{OH})_2$ and $\text{Mg}(\text{OD})_2$ Bands

$\text{Mg}(\text{OH})_2$	$\text{Mg}(\text{OD})_2$	$\text{Mg}(\text{OD})_2/\text{Mg}(\text{OH})_2$
2.30 μ	3.25 μ	1.41 \pm 0.03
2.48	3.43	1.38 \pm 0.03
2.73	3.73	1.37 \pm 0.03
3.07	4.35	1.42 \pm 0.04

One notes from Fig. 13 that the relative intensities among the bands in the spectrum of powdered $\text{Mg}(\text{OD})_2$ (Fig.13) are not quite the same as in the $\text{Mg}(\text{OH})_2$ powder spectrum (Fig. 9(b)). The strong central band at 3.73μ for $\text{Mg}(\text{OD})_2$ is more intense than the 2.73μ band for $\text{Mg}(\text{OH})_2$ relative to the other bands in the complex.

The small band at approximately 1.86μ can be assigned as the overtone of the strong 3.73μ band in the spectrum of $\text{Mg}(\text{OD})_2$.

3.6 Brucite Spectrum, Sections Normal to Cleavage Plane

The spectrum of a brucite section, roughly 250μ thick,

cut perpendicular to the cleavage planes is given in Fig. 14(a). The sample used was prepared using a mixture of optical pitch and bees wax to fasten the brucite during grinding (see 2.3). This mixture has strong bands at approximately 3.45μ , 3.55μ , 5.85μ , and 6.85μ . Small amounts of the mixture were not completely dissolved by the acetone, and these bands appear weakly in the spectrum (marked with crosses). However, these do not interfere with the principal bands of brucite, although the 3.45μ band of the mixture does fall on top of a very weak band of the sample at the same wave length (see Fig. 8).

All the bands that were in the spectrum of the crystal oriented with its c-axis normal to the incident electric vector (Fig. 8) are also present for this orientation (i.e. c-axis parallel to the electric vector). In addition, of course, the band near 2.73μ and its overtone at 1.37μ are present. While the NaCl prism gives poor resolution at short wave lengths, a reproducible shoulder is shown on the short wave length side of the 1.37μ band near 1.33μ . Also, the intensity of the band near 2.30μ is greater relative to all others for this orientation. The band at approximately 2.10μ has been brought out more clearly. A new band has appeared at 3.73μ , and the dip commencing near 6μ is considerably more pronounced.

The polarized spectra are given in Fig. 14(b). The overtone band at 1.37μ and its accompanying shoulder are

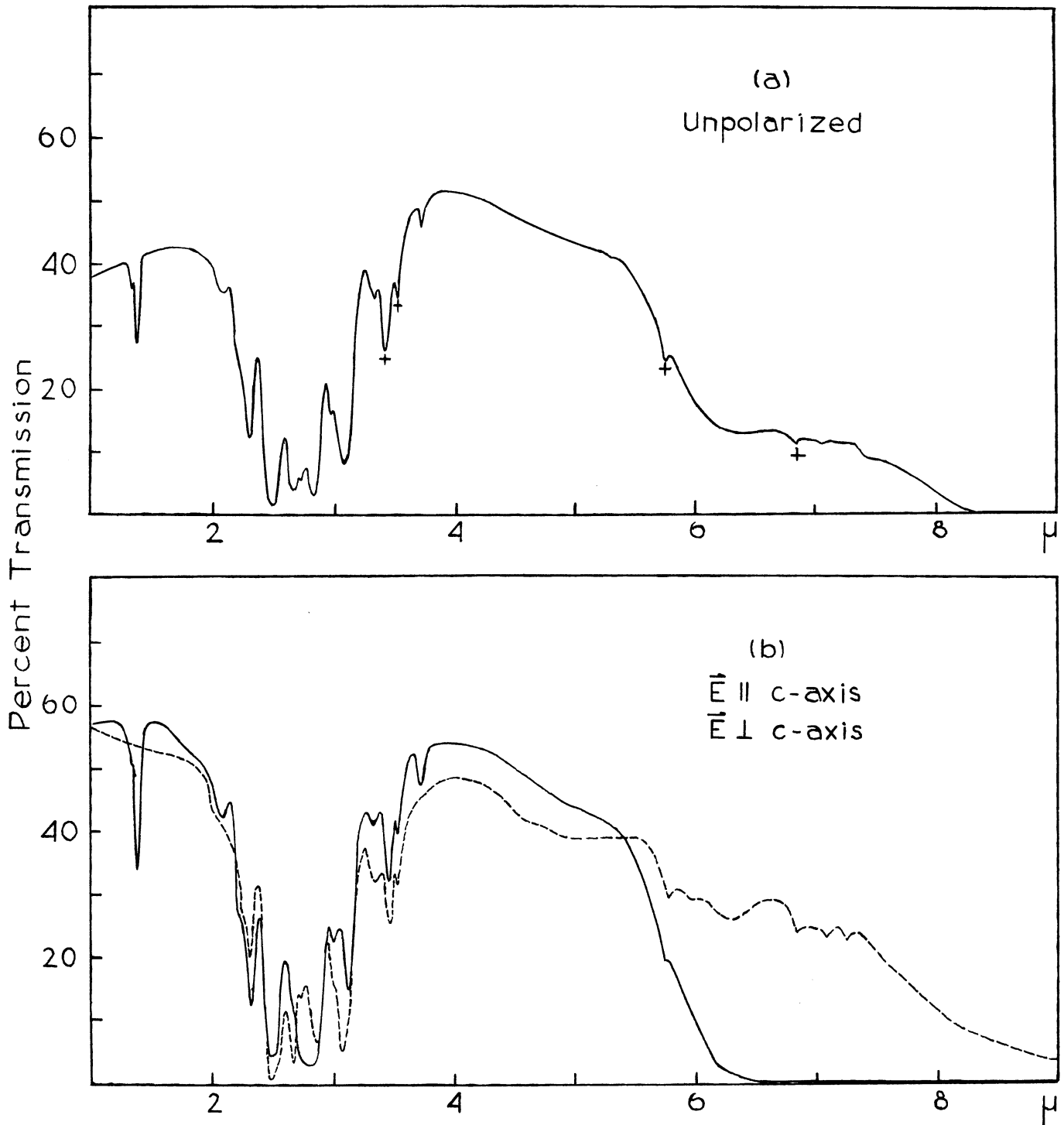


Fig. 14. Spectra of Brucite Crystal 250 Microns Thick (a) with Incident Beam Perpendicular to the c-axis, and (b) with the Electric Vector Polarized Parallel and Perpendicular to the c-axis (NaCl).

completely polarized, i.e. they exhibit maximum absorption when the electric vector is parallel to the c-axis, and they are entirely missing when the electric vector is perpendicular to the c-axis. The same is true for the fundamental at 2.73μ , which is the natural extension of the spectra described in 3.3.

In addition, the weak band at 3.73μ has the same polarization character as the 2.73μ band, i.e. it has never been observed for crystals oriented with their c-axes normal to the incident electric vector. It may perhaps be worth noticing that the 3.73μ band in the spectrum of $\text{Mg}(\text{OH})_2$ is at the same wave length as the strongest band in the $\text{Mg}(\text{OD})_2$ spectrum.

The polarization that occurs for the diffuse band commencing near 6μ is also fairly complete, at least to 8μ . When the electric vector is parallel to the c-axis, the crystal is opaque beyond approximately 6.5μ .

The polarized spectra of the 2μ to 3.25μ region is reproduced on a larger scale in Fig. 15. The main features are that the 2.30μ , 2.73μ , and probably the 2.83μ bands exhibit their maximum intensities when the electric vector is parallel to the c-axis. The 2.48μ , 2.65μ , and 3.07μ bands are polarized in the opposite direction, i.e. they have their maximum absorption when the electric vector is normal to the c-axis. Furthermore, there is a marked shift in wave length of the band in the neighborhood

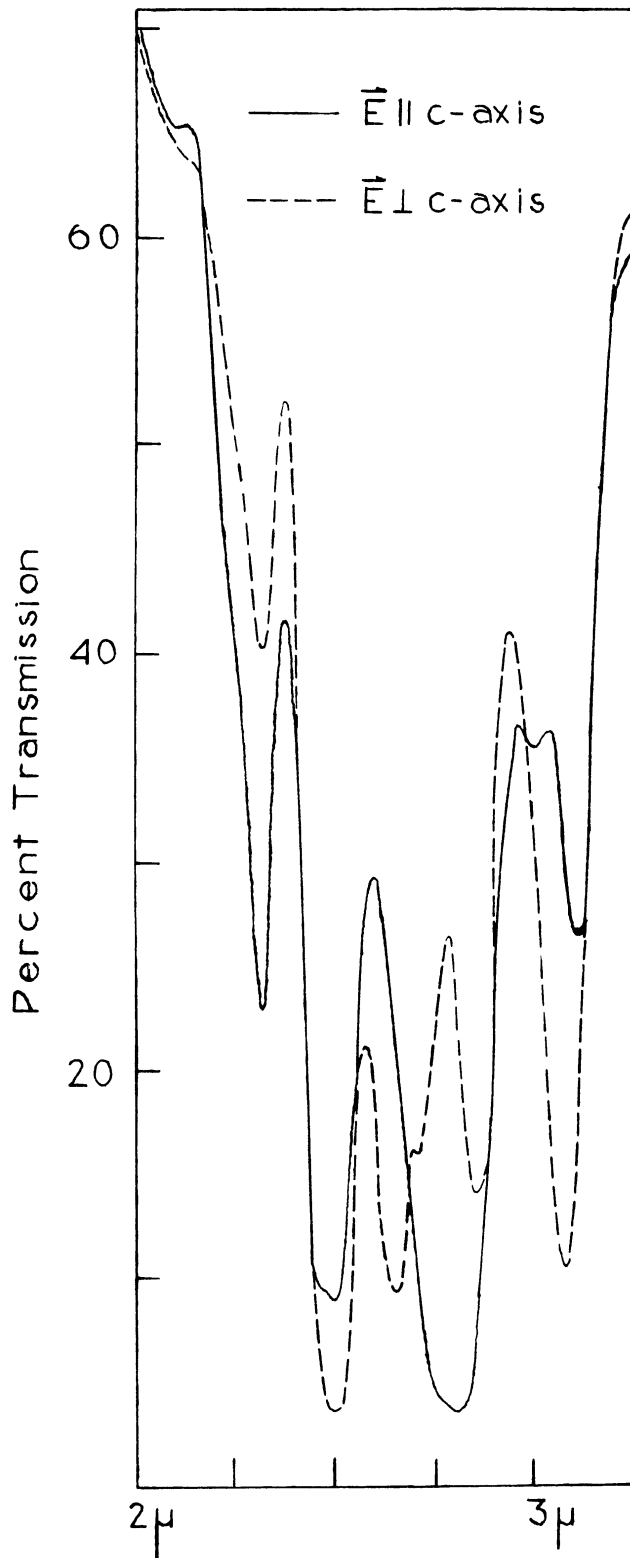


Fig. 15. Spectra of Brucite Crystal 250 Microns Thick with Incident Beam Normal to the **c**-axis and Electric Vector Polarized Parallel and Perpendicular to the **c**-axis (NaCl).

of 3.07μ for the two polarization directions, and the contour of the 2.48μ band is different in the two curves. The fact that the weak 3μ band is missing for one polarization direction may be due to the increase of intensity and the shift in wave length of the 3.07μ band, which then obscures the weak absorption peak.

The spectra shown in Figs. 14 and 15 are independent of the kind of section that is cut normal to the cleavage planes, i.e. all sections cut parallel to the c-axis give the same spectra.

3.7 Spectra of Brucite at High and Low Temperatures

The comparison of the 2μ to 3.5μ brucite spectra at room temperature and in the neighborhood of 350°C is given in Fig. 16. Spectra were recorded at approximately 50° intervals up to 475°C . The crystal was oriented with the c-axis perpendicular to the electric vector. Since there is a great deal of overlapping of these bands even at room temperature, it is impossible to be certain of any quantitative estimates of the variation in relative intensities with temperature. That the overlapping is intensified with increasing temperature can be seen immediately from Fig. 16. However, some rough calculations of the peak intensities are given in Table 5. The 100% transmission line used in each case was a straight line connecting the relatively smooth sections of the curve at slightly less than 2μ and 4μ .

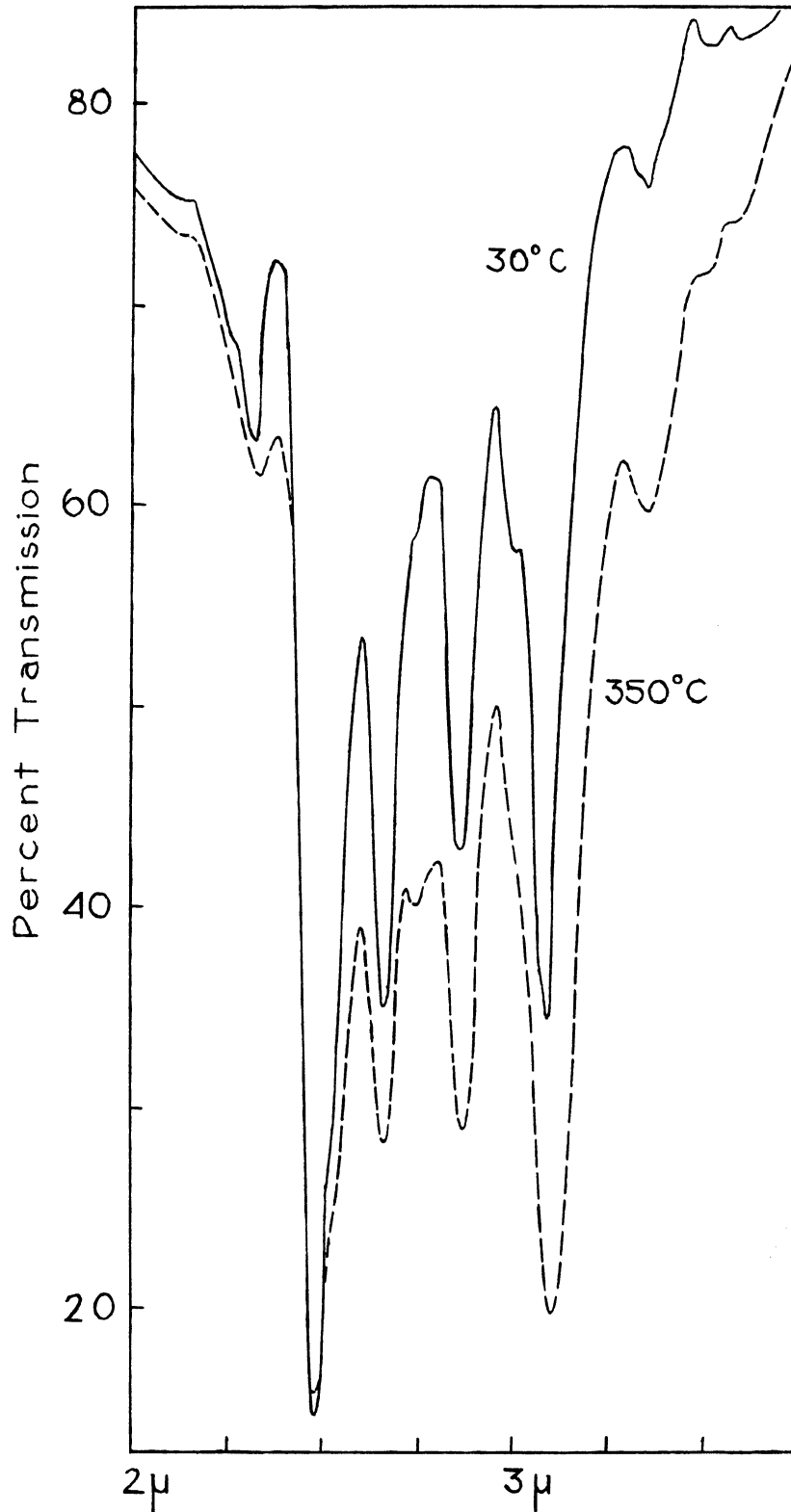


Fig. 16. Spectra of Brucite Crystal with c-axis Parallel to Incident Beam at 30°C and 350°C (NaCl).

Table 5

Intensities of Brucite Bands at 30°C and 350°C

μ	Percent Transmission at 30°C	Percent Transmission at 350°C	Optical Density at 30°C	Optical Density at 350°C
2.48	18	19	1.71	1.66
2.65	42	35	0.87	1.05
2.83	52	35	0.67	1.05
3.07	41	24	0.89	1.43

These values are not to be taken too seriously, since the overlapping of neighboring bands certainly contributes to the peak intensity of each. Also, the broadening of a band due to elevated temperature may cause any spectrometer with less than infinite resolving power to record a higher peak intensity. Keeping these reservations in mind, it may still be noted that the portion of the spectrum at wave lengths beyond approximately 2.6 μ have evidenced the greatest change with increasing temperature. Whether this is due to a relatively larger increase of the true intensities of the 2.65 μ , 2.83 μ and 3.07 μ bands is still somewhat of a question. It is seen, however, that while the peak intensity near 2.48 μ does not change markedly, the shoulder on the long wave length side of this absorption appears further down on the band for higher temperature. The apparent enhancement of the weak band near 2.73 μ in the high temperature spectrum may be largely due to the contributions of the neighboring bands, especially the one on the short

wave length side.

It has been reported that $\text{Mg}(\text{OH})_2$ begins to decompose for temperatures above 350°C ³. The decomposition occurs with the evolution of H_2O leaving behind MgO . However, the brucite spectrum did not change appreciably when the sample was maintained in the temperature range of 370°C to 390°C for approximately twenty hours. This may be due to the fact that the sample was in the form of relatively large crystals instead of a powder. However, when the temperature was progressively increased to 425°C , changes began to occur over a seventeen hour period, in that the intensity of all bands in the 2μ to 3μ region decreased. An additional eight hours at 475°C caused the bands to disappear entirely. No single band decreased in intensity more rapidly than the others over the time that decomposition was taking place. In all, seventeen spectra were recorded over the approximately sixty hours that the sample was being heated. A periodic check was made of the emitted radiation from the heated sample and cell. No appreciable emission was noted in the 2μ to 3μ range for temperatures below roughly 425°C . For higher temperatures, the intensity of the emitted radiation simply increased monotonically with wave length, and did not interfere with the absorption spectrum.

When decomposition was complete (i.e. when all the bands in the 2μ to 3.1μ range disappeared) the sample was allowed to cool to room temperature. The sample had

maintained the shape of the original crystal, but it had become a white powdery substance which was opaque to visible light. The material fell apart into a chalky powder at the slightest touch.

Spectra were also obtained at low temperatures, and these are shown in Fig. 17. The coolants used were a dry ice-acetone mixture and liquid air. The actual sample temperatures were in the vicinity of -60°C and -150°C for the dry ice and liquid air coolants respectively. Constructing a 100% line in the same manner as described for the heated spectra, the percent transmissions at the various temperatures were calculated. These values are tabulated in Table 6.

Table 6

Intensities of Brucite Bands at 30°C , -60°C , and -150°C

μ	Percent Transmission			Optical Density		
	at 30°C	at -60°C	at -150°C	at 30°C	at -60°C	at -150°C
2.48	39	40	42	0.94	0.91	0.87
2.65	68	72	81	0.39	0.33	0.21
2.83	79	86	97	0.24	0.15	0.01
3.07	53	81	-	0.64	0.21	-

The spectrum beyond 3μ for -150°C is omitted, because it was impossible to keep atmospheric water vapor from condensing on the cell faces. The resultant water band obscured the region of the 3.07μ band. Also, the spectra in Fig. 17 are superimposed on a sloping background due to the

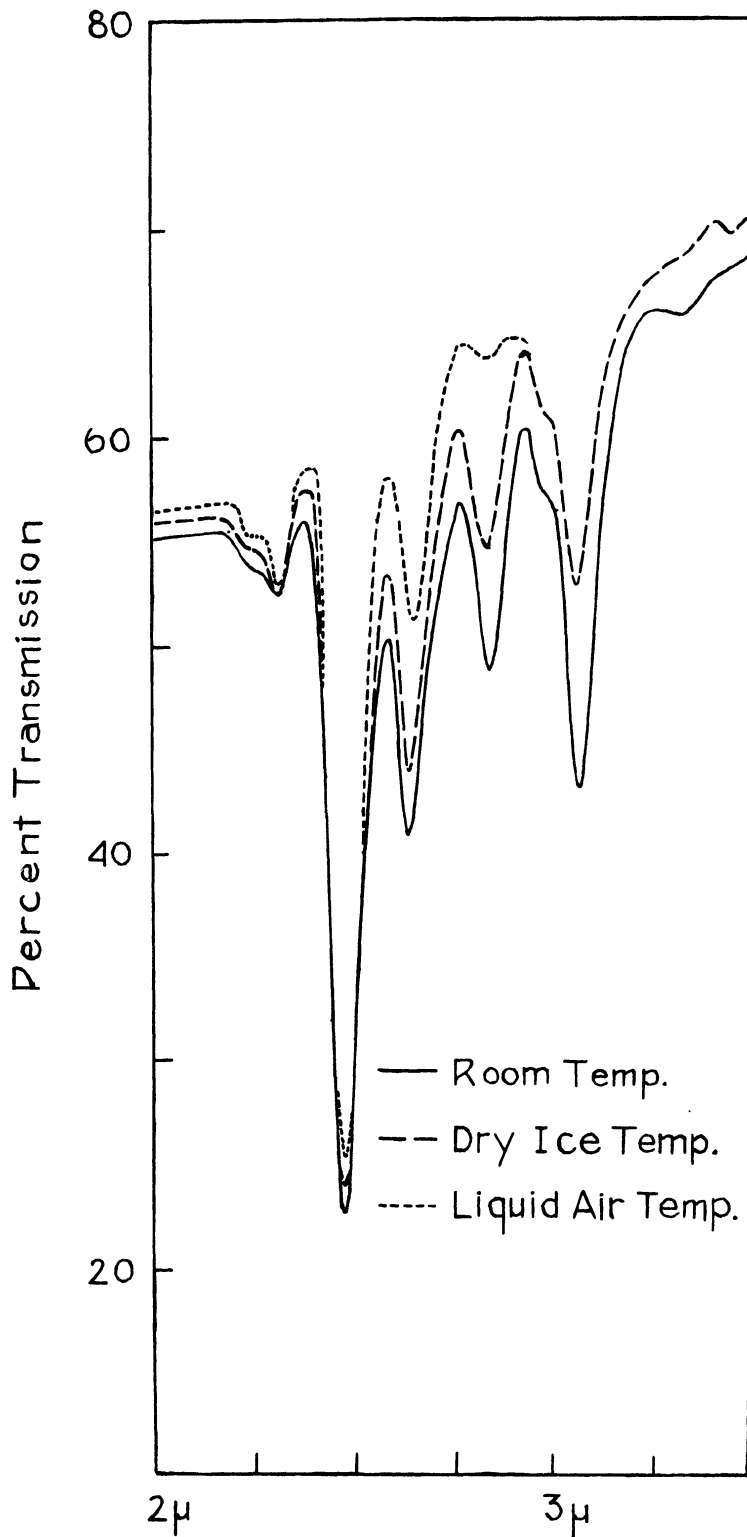


Fig. 17. Spectra of Brucite Crystal with c-axis Parallel to Incident Beam at Room Temperature, Dry Ice Temperature, and Liquid Air Temperature (NaCl).

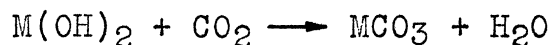
scattering of the AgCl windows on the cold cell. This gives the illusion that some of the relative intensities are different from those in the spectra previously given. While the values in Table 6 cannot be considered as an accurate measure of the relative intensities, it is obvious that the 2.65μ , 2.83μ , and 3.07μ bands are decreasing in intensity with decreasing temperature. It is impossible to say how much the condensation affected the spectrum run near liquid air temperature, but the band composed of both the water and brucite absorptions just beyond 3μ was less intense than the 3.07μ brucite band alone near dry ice temperature. Also, its peak was displaced to approximately 3.10μ . Hence, it would appear that a further decrease in the intensity of the 3.07μ band occurred when the temperature was reduced to about -150°C , but the extent of the decrease could not be determined.

As was the case for the heated spectra, those bands at wave lengths longer than 2.6μ seem to be more sensitive than the others to temperature changes. Also, it is noted that the 2.48μ band becomes narrower with decreasing temperature, and this narrowing takes place predominantly on the long wave length side of the band. It was seen previously that a shoulder on this side increased with increasing temperature.

3.8 Carbonate Impurity in Powdered Samples

In Sections 3.3, 3.4, and 3.5, powdered spectra of

Mg(OH)₂, Ca(OH)₂, and Mg(OD)₂ were described. Those which were chemically prepared were never permitted to come in contact with the atmosphere, and the powdered brucite crystal was put into a nitrogen atmosphere as quickly as possible. This procedure was absolutely necessary, because these hydroxides turn into carbonates when left in the presence of CO₂.²³ The chemical reaction is as follows, where M is the symbol for the metal ion.



This is graphically shown in Fig. 18. Curve (a) is the spectrum of powdered brucite which has been exposed to the atmosphere for several days. The 2.73μ band of the Mg(OH)₂ spectrum is present, but its intensity has been greatly reduced (see Fig. 9(b)). Also, new bands have appeared at roughly 2.95μ, 6.1μ, 6.75μ, 7.05μ, 11.3μ, and 11.7μ. Curve (b) is the spectrum of chemically pure MgCO₃. The similarity between these two curves can leave no doubt that the Mg(OH)₂ has been very largely converted to MgCO₃.

In Section 3.3, the powder spectrum of Mg(OH)₂ between 2μ and 3.2μ was described. The powder used for Fig. 9(b) was in contact with the atmosphere for only two or three minutes. The finer grinding was done in a nitrogen atmosphere. Curve (c) is a spectrum of brucite powder in a fluorolube mull over the region of the strong MgCO₃ absorption. It is noted that no MgCO₃ bands appear when the sample is kept from the atmosphere. Brucite

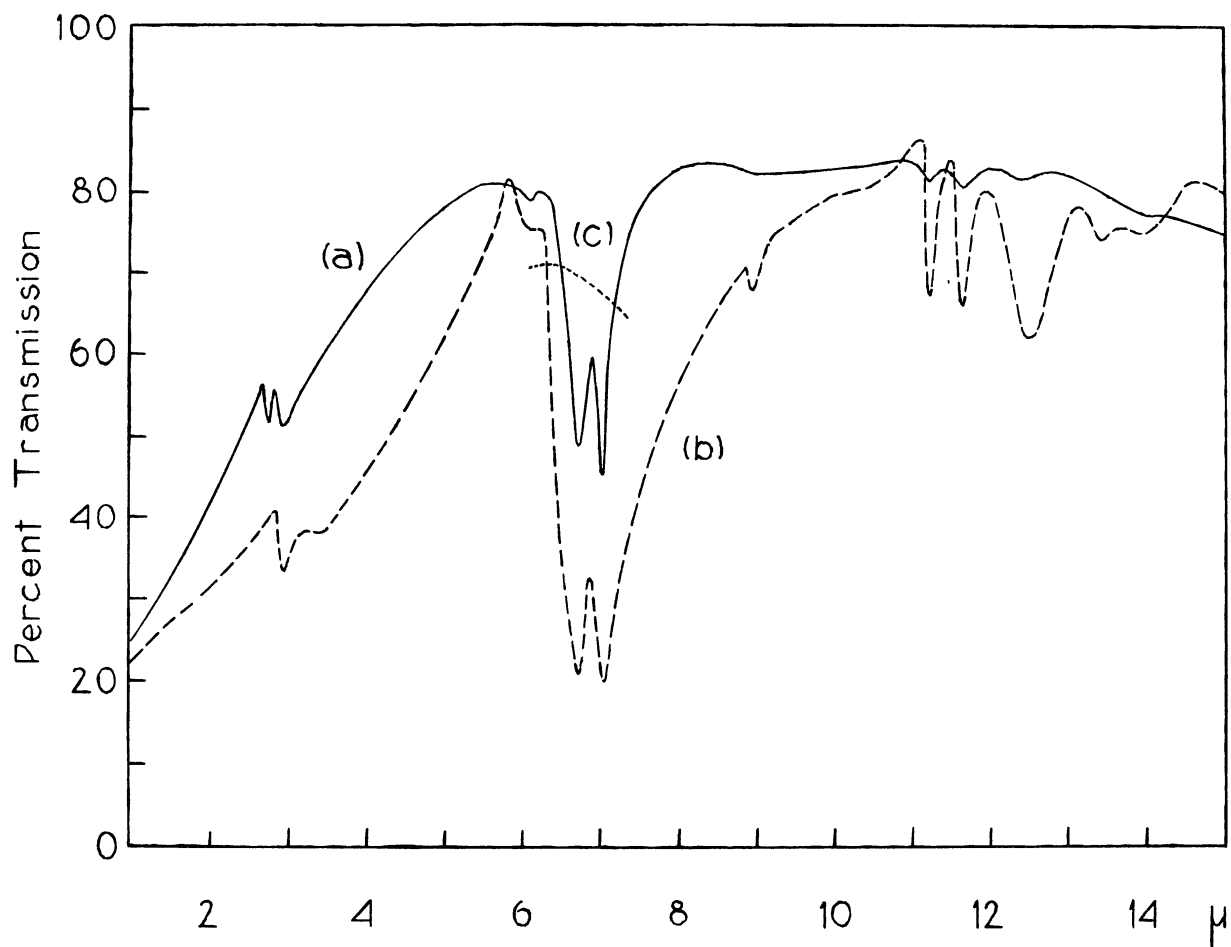


Fig. 18. Spectra of (a) Finely Powdered Brucite which has been Exposed to Air, (b) Chemically Pure $MgCO_3$ Powder, and (c) Finely Powdered Brucite, Not Exposed, in Fluorolube Mull (NaCl).

crystals may be kept in the open air indefinitely without the carbonate being formed to any appreciable degree.

3.9 Increased Resolution, 2μ - 3.2μ Region

All the spectra reported above were obtained with a rock salt prism. The resolution of a rock salt prism is rather poor for wave lengths below 4μ . The University of Michigan spectrometer is equipped with a lithium fluoride prism which gives better resolution in the shorter wave lengths. While this instrument was not operating at its optimum performance, it enabled us to resolve clearly bands separated by only 33 cm^{-1} at approximately 4000 cm^{-1} (2.5μ) which were not resolved with the rock salt prism.

The discussion of the absorption bands which appear in the various spectra given below will always begin with the short wave length bands and progress toward the higher wave lengths.

3.9a Spectrum in 2μ to 2.6μ Region

Under the higher resolving power, several new bands were found near 2.30μ and 2.48μ . These are shown in Fig. 19. The spectra are given for the c-axis of the crystal oriented parallel and perpendicular to the incident beam (I_0).

The samples used were not the same thickness, being

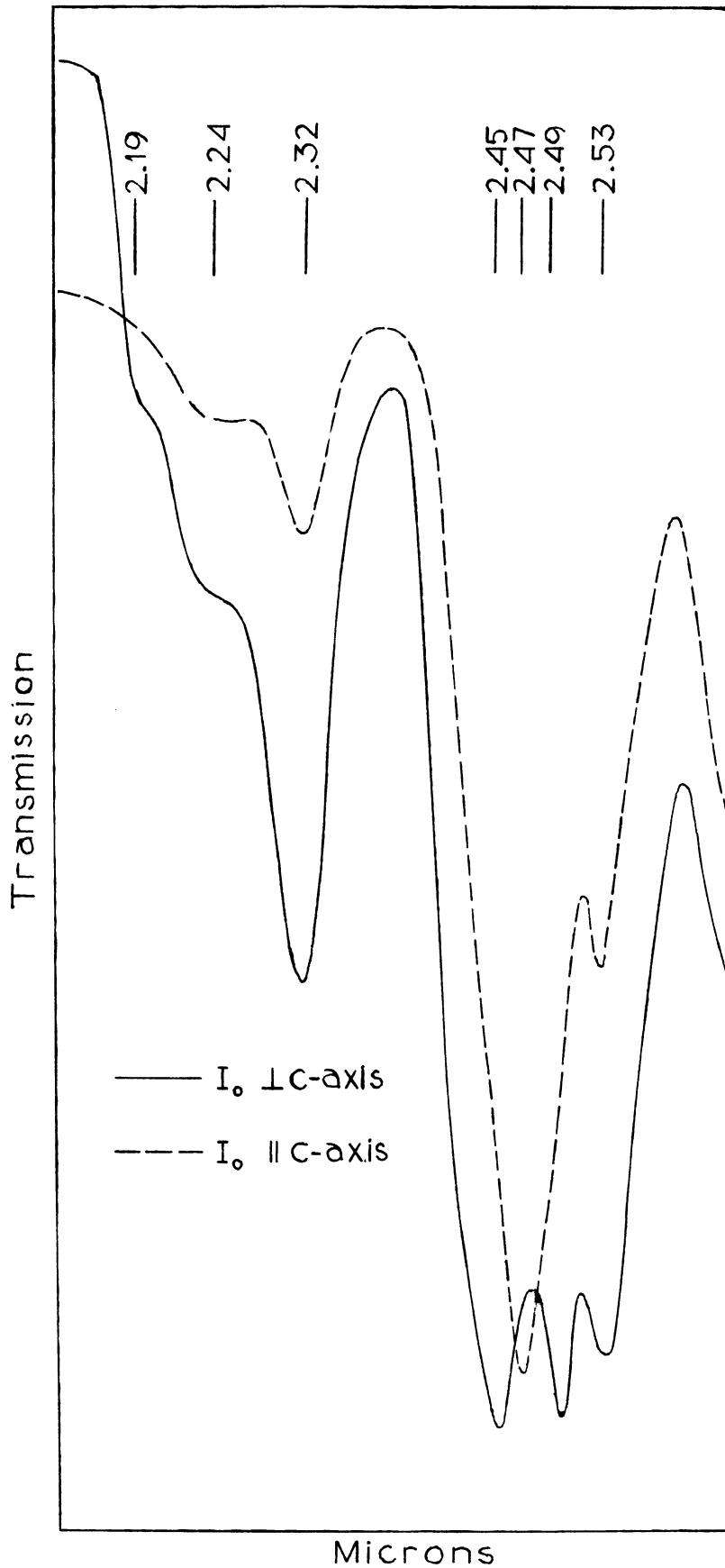


Fig. 19. Spectra of Brucite Crystals 150 and 250 Microns Thick Oriented with c-axis Parallel and Perpendicular to Incident Beam (LiF).

roughly 150μ and 250μ thick for the incident beam being respectively parallel and perpendicular to the c-axis. One notes two shoulders on the short wave length side of the 2.32μ absorption maximum located at 2.19μ and 2.24μ . The complexity of the band centered near 2.5μ explains much that was merely hinted at with the rock salt prism spectra (Fig. 9, 11, 14, 15). Four distinct absorption peaks make up this band, those at 2.47μ and 2.53μ appearing when the incident beam is parallel to the c-axis, and those at 2.45μ , 2.49μ , and 2.53μ appearing when the incident beam is normal to the c-axis. It is reasonable to assume that the band at 2.53μ is responsible for the shoulder that the rock salt prism showed on the long wave length side of this absorption (Figs. 11 and 16).

With the crystal oriented with its c-axis parallel to the incident beam, spectra were taken with the electric vector oriented at all possible angles. Even with the increased resolution, no polarization properties were noted.

However, when the c-axis is oriented normal to the direction of the incident light polarization properties are observed, Fig. 20. The sample used was the same as that used for the spectrum in which the c-axis was normal to the beam in Fig. 19. The intensity of the 2.19μ shoulder is greatly enhanced for the electric vector parallel to the c-axis, as is the 2.32μ band. The polarization

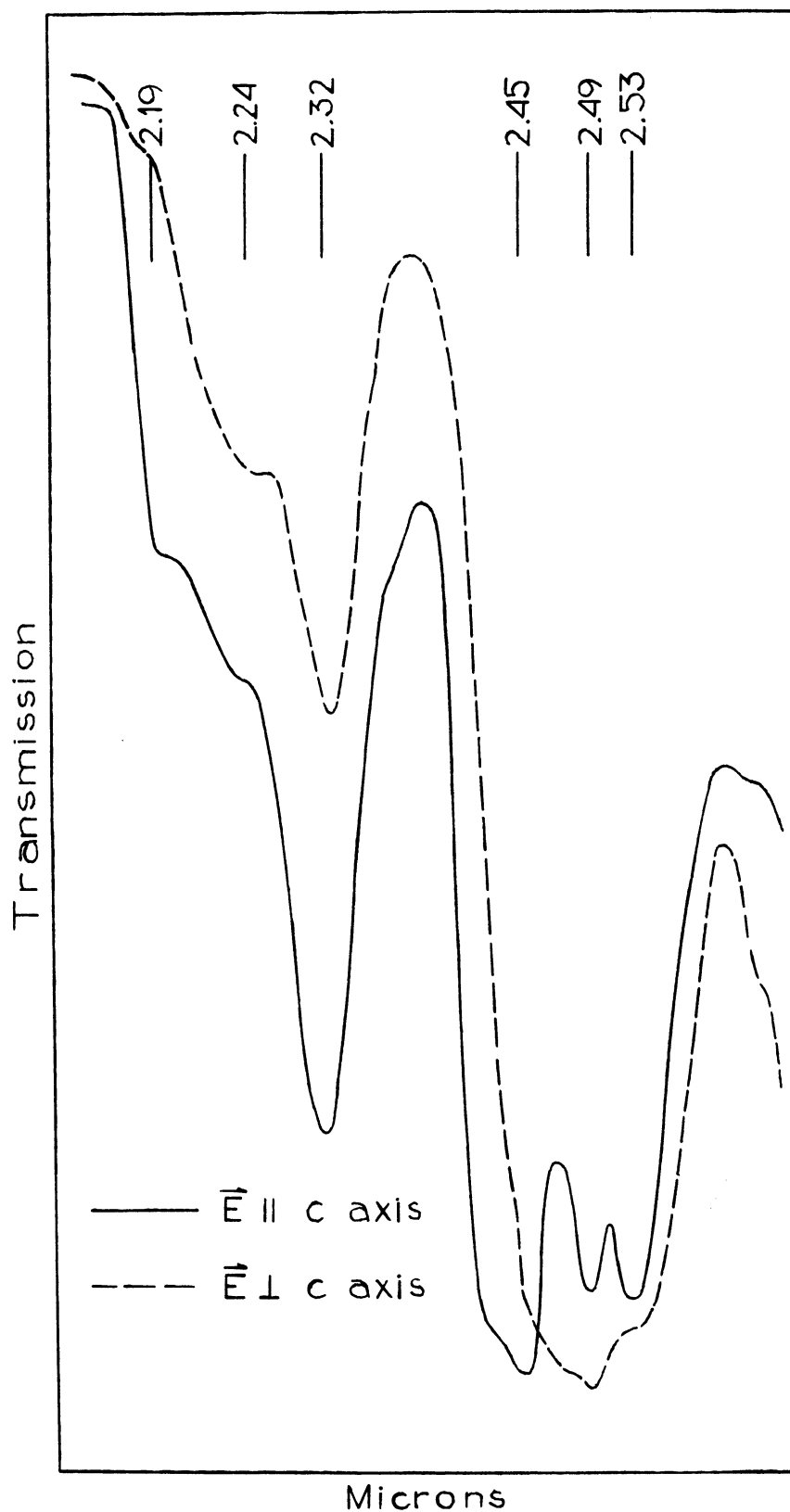


Fig. 20. Spectra of Brucite Crystal 250 Microns Thick with Electric Vector Parallel and Perpendicular to the c-axis (LiF).

properties of the 2.49μ and 2.53μ bands are difficult to determine from Fig. 20. The contour of the entire absorption about 2.5μ and the positions of the absorption maxima are very sensitive to the orientation of the crystal. Four distinct absorption maxima were resolved in this region (Fig. 19). The band at 2.53μ is present when the electric vector is both parallel and perpendicular to the c-axis, while the 2.47μ absorption maximum is observed only when it is perpendicular to the c-axis, and the 2.45μ and 2.49μ peaks appear only when it is parallel to the c-axis. This does not imply that the polarization properties just described are perfect. In all likelihood they are not, i.e. it is likely that all four bands actually occur for both polarizations but with varying relative intensities. The spectra in Fig. 19 indicate that the 2.45μ and 2.49μ bands are polarized with the electric vector parallel to the c-axis. At first sight the curves in Fig. 20 might lead one to the opposite conclusion with regard to the 2.49μ band, unless care is taken in the interpretation. The anomalously high intensity of the 2.49μ component when the electric vector is perpendicular to the c-axis is due to the fact that the 2.47μ band is greatly enhanced. This difficulty can be cleared up by considering an orientation of the crystal which is intermediate between the c-axis being parallel and perpendicular to the incident beam. This situation is pictured in Fig. 21.

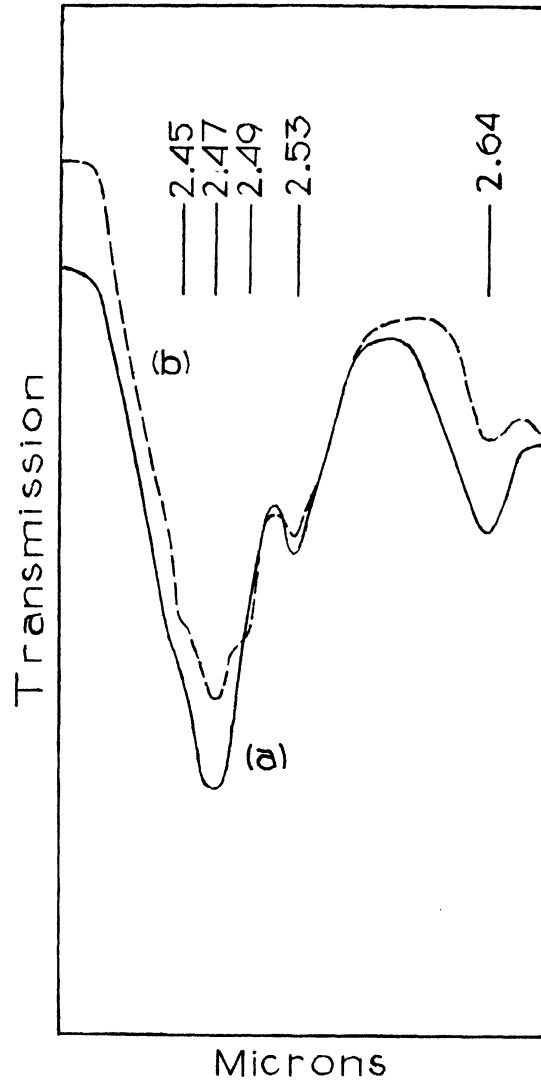


Fig. 21. Spectra of Brucite Crystal with c-axis at 60° to Incident Beam (a) Unpolarized, and (b) Electric Vector Parallel to Plane Defined by c-axis and Incident Beam (LiF). (Sample 50 Microns Thick)

The sample was a cleaved section roughly 50μ thick with its c-axis inclined at an angle of approximately 60° to the incident beam. The full curve shows the unpolarized spectrum of the sample in this orientation. The 2.47μ peak is clearly present with little indication of any structure. The broken curve is the spectrum of the same sample in the same orientation, but with the incident light polarized in a plane defined by the c-axis of the crystal and the direction of the incident beam. The shoulders at 2.45μ and 2.49μ are not clearly exhibited. Since these two shoulders cannot be detected in any way when the c-axis is parallel to the incident beam, it can only be concluded that the intensities of the 2.45μ and 2.49μ bands are enhanced as the component of the electric vector parallel to the c-axis is increasing. Thus, Fig. 20 is misleading with regard to the 2.49μ band, which is in fact polarized with the electric vector parallel to the c-axis. The curves in Fig. 20 are misleading in the same way with regard to the polarization of the 2.53μ band. Actually, this is also polarized with the electric vector parallel to the c-axis.

3.9b Spectrum in 2.8μ to 3.2μ Region

In Fig. 22 are shown the spectra from 2.8μ to 3.2μ of the same two samples as were used for Fig. 19. One notes that the band at 2.83μ is not resolved into more than one component with

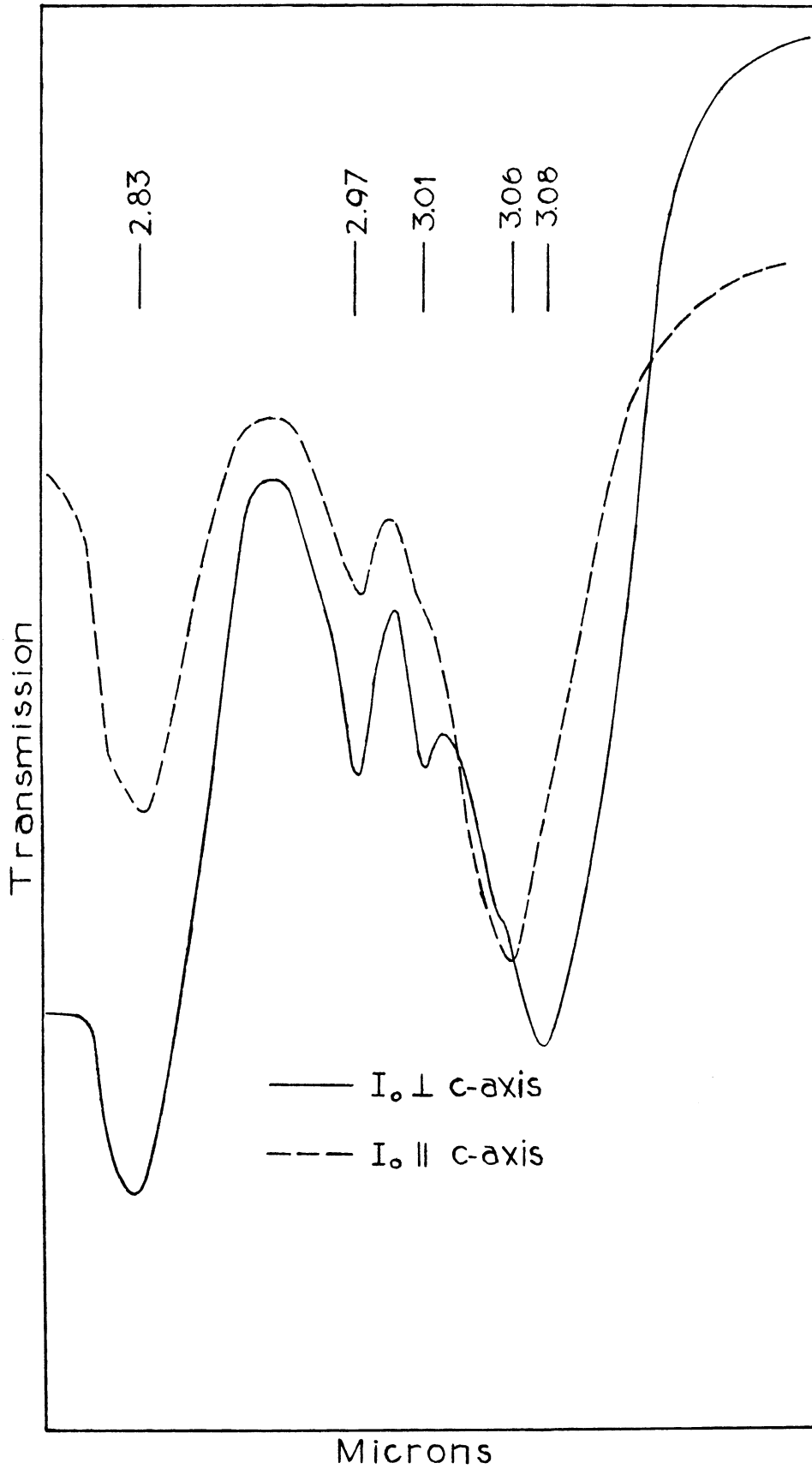


Fig. 22. Spectra of Brucite Crystals 150 and 250 Microns Thick Oriented with c-axis Parallel and Perpendicular to Incident Beam (LiF).

the higher dispersion, although there is some hint of a shoulder on the short wave length side. A weak band at 2.97μ is clearly resolved in both spectra, while a weak band at 3.01μ is resolved in the curve for the c-axis normal to the beam but appears only as a shoulder for the other orientation. A band is observed near 3.07μ , whose peak intensity is at 3.06μ when the c-axis and the incident beam are parallel. For the other orientation, the peak has shifted to 3.08μ , and only a shoulder is present at 3.06μ .

No dichroism was observed over this region of the spectrum when the incident beam was parallel to the c-axis. The polarized spectra for the incident beam normal to the c-axis are shown in Fig. 23. As was the case with a rock salt prism (Fig. 15), it is difficult to say with certainty if the 2.83μ band is polarized at all, because when the electric vector is parallel to the c-axis the peak of this band is obscured by the strong absorption near 2.73μ .

The polarized spectra of the bands at 2.97μ and 3.01μ are in agreement with the orientation spectra in Fig. 22.

The high resolution polarized spectra verify the shift in position that was noticed for the absorption near 3.07μ using a rock salt prism (see 3.6). It is also in agreement with the orientation spectra shown in Fig. 22.

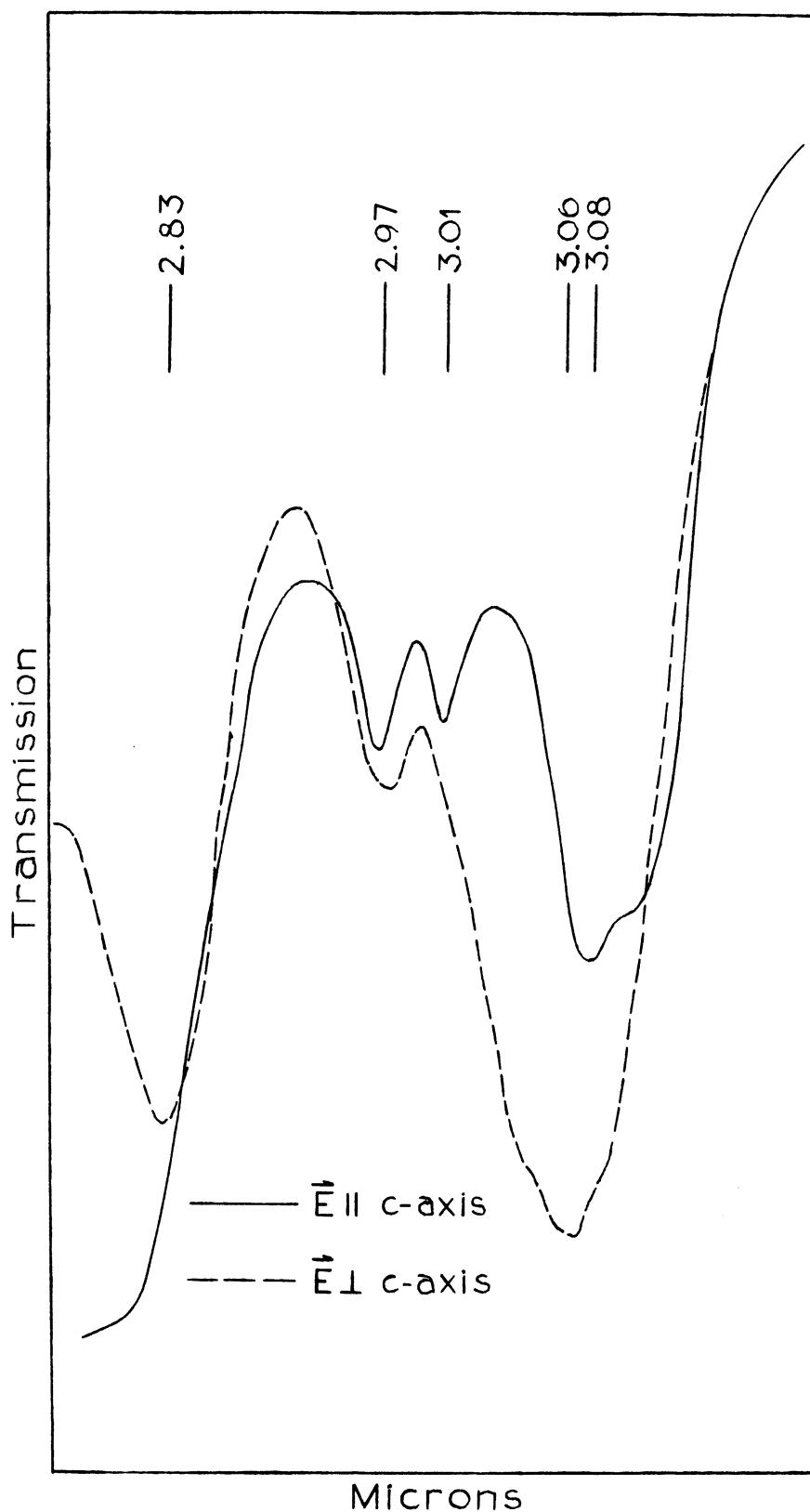


Fig. 23. Spectra of Brucite Crystal 250 Microns Thick with Electric Vector Polarized Parallel and Perpendicular to the c-axis (LiF).

A band whose center is at 3.08μ is observed when the electric vector is parallel to the c-axis, while when the electric vector is perpendicular to the c-axis, the band center shifts to 3.06μ and the intensity is increased considerably. There are further indications of possible structure in these bands, somewhat in the manner of the absorption near 2.5μ , but no further absorption maxima have been resolved.

3.9c Spectrum in 2.6μ to 2.8μ Region

The University of Michigan spectrometer can deliver very little energy to the thermocouple in the range 2.7μ to 2.8μ . As described in 2.1, this is due to the extremely long optical path length in the instrument (resulting in high atmospheric absorption) and to an impurity in the LiF prism (causing a strong absorption near 2.8μ). For this reason, the spectrum of the 250μ thick sample which was cut perpendicular to the cleavage plane gave no information in this region. The strong absorption of the brucite in this low energy interval made the spectrometer sluggish and unresponsive. This was even more pronounced for polarized spectra, where the polarizer reduced the energy by another factor of two.

It was still possible to take advantage of the higher resolution of this instrument over the 2.6μ to 2.8μ region. A cleaved specimen approximately 50μ thick was oriented

with its c-axis at three different angles to the incident beam. The spectra at these angles are shown in Fig. 24. When the c-axis is parallel to the incident beam, a band appears at 2.63μ , and a weak sharp band is observed at 2.71μ . No dichroic properties were observed for this orientation. When the c-axis is tilted to approximately 45° , the intensity of the 2.64μ band is somewhat diminished, and polarized spectra for this orientation confirm the rock salt spectrum (Fig. 15) in that this band exhibits maximum absorption when the electric vector is perpendicular to the c-axis.

Variations with orientation are also noticed in the 2.7μ to 2.75μ region. When the crystal is tilted to approximately 45° , a stronger absorption is observed in this neighborhood. The band now exhibits a shoulder at 2.74μ , and the peak absorption has been shifted to 2.72μ . For an angle near 60° , the intensity of the absorption has increased further, and the shoulder is almost at the peak intensity of the entire absorption. Unfortunately, it was not possible to obtain spectra for larger angles due to the limitation of the sample size. Nevertheless, it is apparent that the absorption in this region consists of at least two components at 2.71μ and 2.74μ . It is impossible to say whether a third band is appearing at 2.72μ for the spectra of the inclined crystal, or whether the 2.74μ shoulder overlaps the 2.71μ

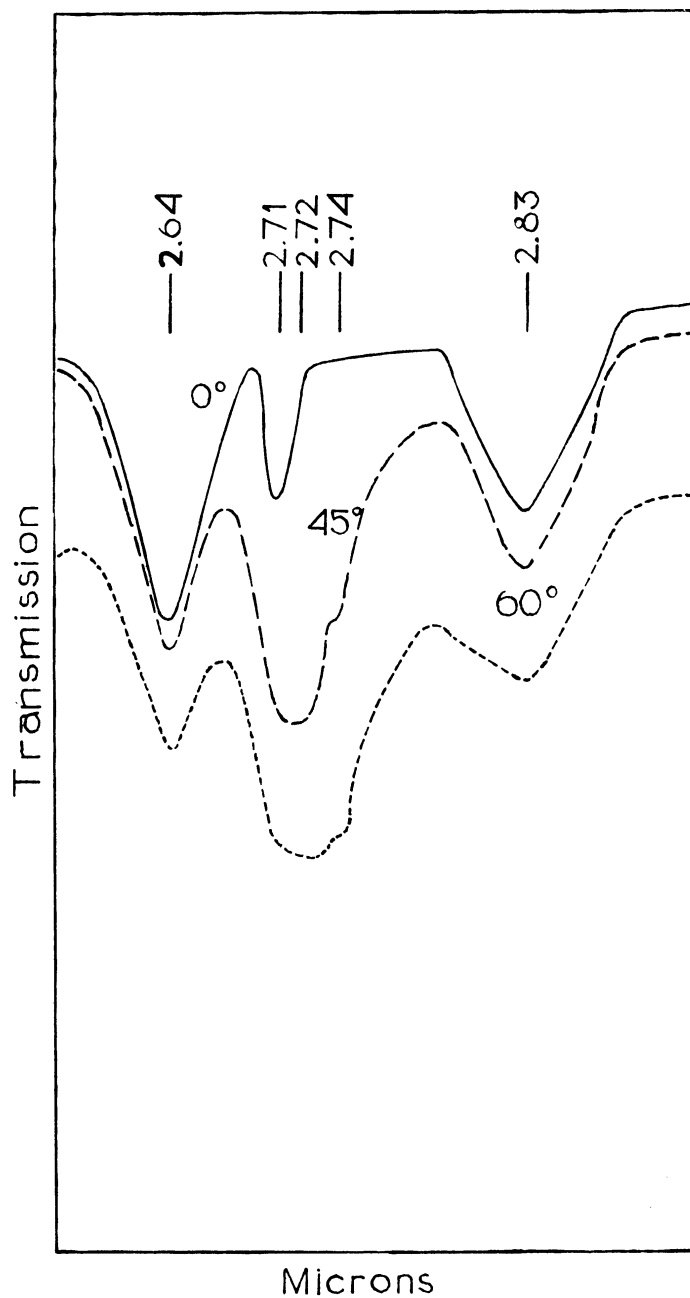


Fig. 24. Spectra of Brucite Crystal with c-axis at 0° , 45° , and 60° to Incident Beam, Sample 50 Microns Thick (LiF).

band sufficiently to shift the peak absorption to 2.72μ .

In either event, we may conclude that the absorption which appears near 2.73μ when the c-axis presents a component to the incident electric vector (Fig. 10) is multiple, i.e. it is composed of at least two distinct bands.

3.10 Brucite Spectrum, 15μ - 33μ Region

The thinnest cleaved brucite crystal we were able to prepare was approximately 15μ to 20μ thick. The spectrum of this sample from 1μ to 15μ was given in Fig. 8(a). A cut-off in the transmission is noted near 14μ . The absorption was investigated to 33μ with a Perkin-Elmer Model 112 spectrometer using a CsBr prism, however, even this thin specimen was completely opaque from 14μ to 33μ .

3.11 Summary

The principal features of the brucite spectrum are an overtone band at 1.37μ , a cluster of relatively sharp bands between 2μ and 3.1μ , a broad shallow band commencing near 6μ , a pair of sharp but weak bands at 7.08μ and 7.23μ , and a strong absorption beginning near 14μ and extending at least to 33μ . The spectrum of brucite is very sensitive to the orientation of the crystal relative to

the incident electric vector. Bands which appear for one orientation may be entirely missing for another, for which new bands may be observed. The positions in microns and wave numbers of all the bands that have been resolved are given in Table 7, along with the orientations for which they appear and their dichroic properties. The orientations used are those for which the crystal c-axis is parallel and perpendicular to the incident electric vector, E. The polarization properties are described as being parallel(P) or normal(N) to the c-axis according as the maximum intensity occurs with the electric vector polarized parallel or perpendicular to the c-axis of the crystal. Those which are further designated with a (c) are completely missing if the incident electric vector is polarized normal to the direction of maximum intensity. In addition, those variations that have been measured of the intensities of bands (or groups of bands) with temperature are given in Table 7. The letters I and D indicate an increase or a decrease of intensity with a raising or lowering of the temperature.

By far the richest portion of the spectrum is from 2μ to 3.1μ . Sixteen bands have been observed in this interval, and there are suggestions of shoulders on the 2.83μ , 3.06μ , and 3.08μ bands.

Table 7

List of Infrared Absorption Bands of Brucite

$\vec{E} \perp$ c-axis	$\vec{E} \parallel$ c-axis			Temperature	Effect
				High T	Low T
	1.33 μ	P(c)	7520 cm ⁻¹		
	1.37	P(c)	7300		
2.06 μ	2.06		4860		
2.19	2.19	P	4565		
2.24	2.24		4465		
2.32	2.32	P	4310		
(2.45)	2.45	P	4082] (D)	D
2.47	(2.47)	N	4049		
(2.49)	2.49	P	4016		
2.53	2.53	P	3952		
2.64	(2.64)	N	3788	I	D
2.71	2.71	P	3690		
	2.74	P(c)	3649		
2.83	2.83	P?	3533	I	D
2.97	2.97		3367		
3.01	3.01		3320		
3.06	3.06	N	3268] I	D
(3.08)	3.08	P	3247		
3.35	3.35		2985		
3.45	3.45		2898		
	3.73	P(c)	2681		
5.00	5.00		2000		
6.25	6.25	P	1600		
7.08	7.08		1412		
7.23	7.23		1383		
8.3	8.3		1205		
9.9	9.9		1010		
14-33	14-33				

The broad band commencing near 6 μ is strongly polarized with the electric vector parallel to the c-axis. This band becomes so strong with this polarization that the cut-off in transmission, which is normally just beyond 8 μ for a sample 250 μ thick, appears to begin near 6.5 μ . The two

bands at 7.08μ and 7.23μ have no polarization properties when the c-axis is parallel to the incident beam, nor do their intensities vary appreciably when the c-axis is inclined with respect to the incident beam. Unfortunately, their polarization properties with the c-axis normal to the incident beam cannot be observed because of the absorption of the band near 6μ .

The powder spectra indicate that the absorptions near 2.30μ , 2.48μ , 2.73μ , and 3.07μ for $\text{Mg}(\text{OH})_2$ are each shifted by $\sqrt{2}$ for $\text{Mg}(\text{OD})_2$. However, the bands of the deuterated compound do not have the same relative intensities as do those of $\text{Mg}(\text{OH})_2$. The strong central absorption at 3.73μ for $\text{Mg}(\text{OD})_2$ is somewhat more intense relative to the rest of the bands in the group than is the case for the 2.73μ absorption for $\text{Mg}(\text{OH})_2$.

When the brucite crystal is heated, the bands near 2.65μ , 2.83μ , and 3.07μ increase in intensity. The shoulder (2.53μ band in LiF spectra) on the long wave length side of the 2.48μ absorption is enhanced with increasing temperature. When the crystal is cooled, the 2.65μ , 2.83μ , and 3.07μ bands are reduced in intensity. The 2.48μ absorption is slightly reduced in intensity also for the low temperature spectra, and the same shoulder (2.53μ band) on the 2.48μ absorption that increases with elevated temperatures decreases in intensity when the temperature is reduced.

CHAPTER 4

Discussion of Experimental Results

4.1 Comparison With Previous Infrared Work

It is apparent that the present work has given much new and detailed information concerning the infrared spectrum of brucite. The most important advance has been made in the 2μ to 3.1μ region, where many of the particulars of the involved absorption complex are now known. The only previous studies reported for this interval are those of Coblenz, Plyler, and Louisfert (whose spectra extended only to 2.5μ), and a review of these papers was given in 1.3 above. The present work is in general agreement with that of Coblenz and Plyler, apart from differences due to the higher resolving power now available. However, there is a definite conflict with the results of Louisfert.

Louisfert reported the presence of bands at 2.14μ , 2.32μ , and 2.46μ when the incident electric vector was perpendicular to the c-axis. However, Louisfert maintained that the 2.46μ band is missing when the electric vector is parallel to the c-axis. That this result is in complete disagreement with our results is shown by Figs. 19, 20, and 21. From these it is clear that the general absorption near 2.5μ is composed of at least four

bands having different dichroic properties, but under no condition are they all absent from the spectrum. Furthermore, the band that Louisfert found at 2.46μ cannot be the 2.45μ component of this absorption, since the 2.45μ absorption maximum appears only when the electric vector is parallel to the c-axis, i.e. its dichroism is exactly opposite to that described by Louisfert. The only explanation that can be offered for this discrepancy is the possibility that Louisfert had her spectra interchanged in some manner. Our results on this point are clear cut and were checked at least three times.

Our experiments are largely in agreement with Yeou Ta, whose results were described in 1.3 above. An absorption band is present near 1.37μ only when the electric vector has a component that is parallel to the c-axis of the crystal. However, our spectra indicate the presence of a shoulder on this band near 1.33μ , whose properties are the same as the 1.37μ band. Yeou Ta mentioned the appearance of only one band, and since he gave no curves with his paper, it is impossible to know if he observed this shoulder. While our resolving power at this wave length was very low, the presence of the shoulder was quite marked, and its contour was reproducible (see Fig. 14).

While Yeou Ta described only the properties of the overtone band, we were able to examine the fundamental

region also. However, there is some difficulty in deciding which band is the fundamental of the 1.37μ band. Indeed, there is some doubt that the 1.37μ band is a single frequency itself. The difficulty can best be described by a brief review of some of the high resolution experimental results. The curves in Fig. 24 show the 2.7μ to 2.75μ region of the spectrum for the c-axis oriented at various angles to the incident light. When the electric vector is normal to the c-axis, the only absorption in this interval is a weak sharp band at 2.71μ . The intensity of this band increases when the specimen is inclined so that the electric vector has a component parallel to the c-axis, and at the same time a new band appears at 2.74μ whose intensity is also enhanced with further tilting of the crystal. (As remarked in 3.9, it is impossible to say whether a third band is appearing at 2.72μ or whether the overlapping of the 2.74μ band is shifting the position of the peak intensity to 2.72μ . It is sufficient for the sake of this argument to assume that only the two bands are present.) Thus we see that the absorption which appears in this region when the electric vector has a component parallel to the c-axis (see Fig. 10) is composed of at least two distinct bands at 2.71μ and 2.74μ . Since overtone bands are generally not at exactly twice the frequency of the fundamental, and since the bands at 2.71μ and 2.74μ have almost identical properties,

there is no way of definitely assigning the fundamental in this case. In fact, it is certainly possible that the overtones of both these bands are present in the 1.37μ absorption.

A critical survey of the work of Duval and Lecomte has already been given in 1.3 above, and it is only necessary to remark again that the experimental results described in 3.8 indicate that their powder samples had become contaminated with $MgCO_3$ through contact with the CO_2 in the atmosphere.

4.2 Interpretation of Bands in 2μ - 3.1μ Complex

The mere presence of sixteen bands in the 2μ to 3.1μ interval with intensities of the same order of magnitude leads one to suspect that there are several OH stretching fundamental frequencies in the brucite spectrum. However, this can be established by considering in detail the possible interpretations of the experimental results described in Chapter 3.

One might first ask what these various bands are, if they are not OH stretching fundamental frequencies. It might be supposed that these bands could be assigned as (a) absorptions due to impurities, (b) bands due to water of crystallization, (c) fundamentals associated with modes other than OH stretching, (d) overtones and combinations of low lattice frequencies, (e) combinations of low lattice frequencies with a single OH stretching

fundamental frequency. In the following paragraphs, these possibilities will be discussed, and it will be shown that the complex of absorption bands cannot be explained on these bases.

(a) The fact that chemically pure $\text{Mg}(\text{OH})_2$ gives the same spectrum as powdered brucite (see 3.4) rules out the possibility that any of these bands are due to impurities in the natural mineral.

(b) None of the stronger bands can be due to the presence of water of crystallization, since the associated deformation frequencies near 6.1μ are not observed.¹⁵ It is just conceivable that one of the weak bands at 2.97μ or 3.01μ (Fig. 22) might be due to the OH stretching motion of water of crystallization, if it can be assumed that the 6.1μ band (always somewhat weaker) is too weak to be observed.

One is, therefore, forced to the conclusion that at least fourteen of the sixteen bands in this region are due to the motions of the atoms in the $\text{Mg}(\text{OH})_2$ crystal.

(c) The bands between 2μ and 3.1μ cannot be fundamentals associated with normal modes (other than OH) of the crystal. Knowledge of force constants and their effect on frequency shows that atoms as heavy as oxygen and magnesium do not vibrate with such high frequency. If the simple diatomic molecule MgO existed, then it would have a fundamental stretching frequency at 785 cm^{-1} or 12.7μ ³⁸.

Since all normal modes of brucite, excluding OH modes, are essentially stretching and deformation of the Mg-O bonds, then one would expect that these frequencies would appear at 12.7μ and beyond. This is indeed observed, since a brucite crystal of thickness $15-20\mu$ is opaque from roughly 14μ to at least 33μ (see 3.10).

(d) The bands in the 2μ to 3.1μ interval cannot be overtones of any such lower lattice frequencies. Since the spectrum is relatively clear from 3.1μ to 14μ , they would have to be fourth or higher overtones with all the lower order overtones infrared inactive. Such cannot be the case, because at least alternating orders of overtones must be of the same species and hence the same activity.

Similarly, it seems most improbable that they would be very high order combinations of low lattice frequencies with all lower order combinations missing.

(e) If these bands are not OH stretching fundamental frequencies, then the only remaining possibility is that they are combinations of low lying lattice frequencies with the OH stretching fundamental. One might then suppose that the complex of absorptions in the 2μ to 3.1μ interval consists of sum and difference combinations of low lattice frequencies with a single OH stretching fundamental. If one assumes that a single OH stretching fundamental in the brucite crystal gives rise to the band at 2.74μ or 3649 cm^{-1} (which has its dipole moment change directed

parallel to the c-axis), then it would follow that the other bands between 2μ and 3.1μ are combinations with this frequency. The energy level diagram given in Fig. 25(a) shows the levels and transitions representing such a collection of bands.

There are particular properties of the spectrum that must be observed, if Fig. 25(a) represents the energy level scheme through which these many bands arise. These are examined in the following paragraphs in light of the experimental results given in Chapter 3.

The separations of the various band maxima from the 3649 cm^{-1} (2.74μ) maximum can be computed from Table 7 and are listed below in Table 8.

Table 8

Separation of Brucite Bands from 3649 cm^{-1}

From "Sum" Bands		From "Difference" Bands	
ν	$\nu(L) = \nu - 3649$	ν	$\nu(L) = 3649 - \nu$
4860	1211		
4565P	916		
4465	816		
4310P	661		
4082P	433		
4049N	400	3247P	402
4016P	367	3268N	381
		3320	329
3952P	303		
		3367	282
3788N	139	3533P?	166
3690P	41		

If the bands listed in columns 1 and 3 of Table 8 are sum and difference combinations of low lattice

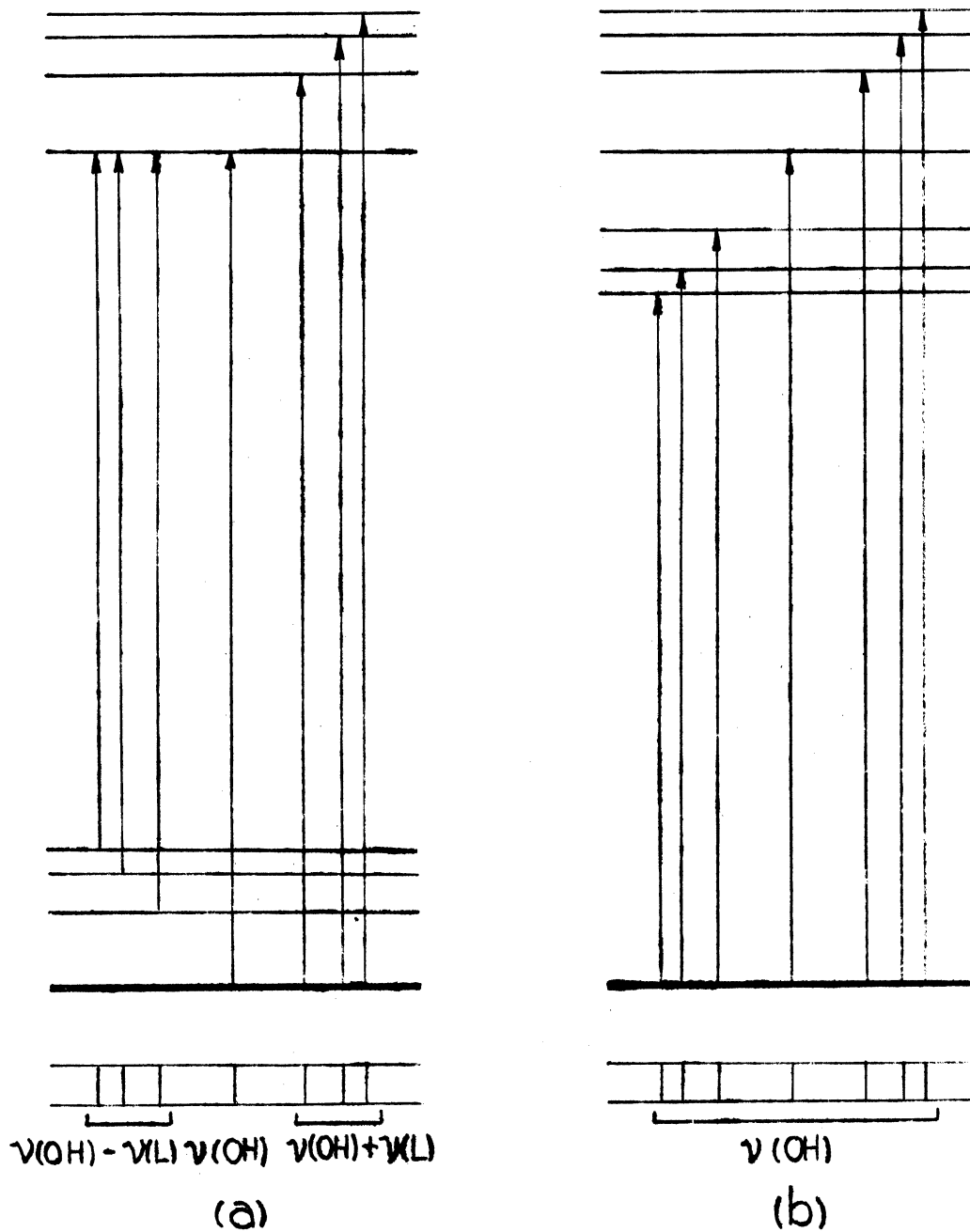


Fig. 25. Energy Level Diagrams to Explain the Absorption Complex in Terms of (a) Sum and Difference Combinations of Low Lattice Modes with a Single OH Stretching Fundamental, and (b) Multiple OH Stretching Fundamentals.

frequencies with the OH fundamental, then the 3788 cm^{-1} (2.64μ), 4016 cm^{-1} (2.49μ), and 4049 cm^{-1} (2.47 cm^{-1}) bands must be the sum bands corresponding to the difference bands at 3533 cm^{-1} (2.83μ), 3268 cm^{-1} (3.06μ), and 3247 cm^{-1} (3.08μ), i.e. these would be the frequencies $\nu(\text{OH}) + \nu(\text{L})$ and $\nu(\text{OH}) - \nu(\text{L})$ where $\nu(\text{L})$ is approximately 150 cm^{-1} , 370 cm^{-1} , and 400 cm^{-1} respectively. However, this cannot be the case, since in each instance the "sum" band has different polarization properties from the corresponding "difference" band (see 3.9 and Table 7), and hence they belong to different species. Sum and difference bands of this kind must have the same polarization properties, since they are of the same species.³⁹

This is shown by the following symmetry argument. If $\Psi(\text{OH})$ and $\Psi(\text{L})$ are the wave functions describing the excited states of the OH fundamental and lattice mode respectively, then the selection rule for the transition $\nu(\text{OH}) - \nu(\text{L})$ depends upon the symmetry of $\Psi(\text{OH})\Psi(\text{L})$. The selection rule for $\nu(\text{OH}) + \nu(\text{L})$ depends only on the symmetry of the upper level, since the transition originates from the ground state. But the wave function $\Psi(\text{OH} + \text{L})$ describing the upper level for $\nu(\text{OH}) + \nu(\text{L})$ has the same symmetry as $\Psi(\text{OH})\Psi(\text{L})$.

It can also be proved that these six bands at 4049 cm^{-1} , 4016 cm^{-1} , 3788 cm^{-1} , 3533 cm^{-1} , 3268 cm^{-1} , and 3247 cm^{-1} cannot be combinations of any low frequency with an OH

fundamental. It has already been shown that if the bands on the low frequency side of 3649 cm^{-1} were combination bands, then they must be combinations of low lattice frequencies with the OH fundamental, i.e. difference bands of the type $\nu(\text{OH}) - \nu(\text{L})$. However, if the difference bands are observed, then the corresponding sum bands must be observed also, since they both obey the same selection rules. But the "sum" bands corresponding to the bands at 3533 cm^{-1} (2.83μ), 3268 cm^{-1} (3.06μ), and 3247 cm^{-1} (3.08μ) are not observed. Therefore, these three bands cannot be difference bands.

Using a similar argument, it can be proved that the bands at 4049 cm^{-1} (2.47μ), 4016 cm^{-1} (2.49μ), and 3788 cm^{-1} (2.64μ) cannot be sum bands. Since the matrix elements $\int \psi''^* M \psi' dt$ are the same order of magnitude for sum and difference combinations³⁹, the factor determining their relative intensities is the relative populations of the low lattice level and the ground state. At room temperature, kT is equivalent in energy to approximately 210 cm^{-1} , which means that the Boltzmann distribution, $\exp(-h\nu/kT)$, as a function of ν has its maximum near 210 cm^{-1} at room temperature. Therefore, any low lying state at approximately 150 cm^{-1} , 370 cm^{-1} , or 400 cm^{-1} would have a significant fraction of the total population, and any allowed transition that originates from one of these low levels should be observed in the spectrum. Hence, if a sum band,

$\nu(\text{OH}) + \nu(\text{L})$, is observed in the spectrum where $\nu(\text{L})$ has the value 150 cm^{-1} , 370 cm^{-1} , or 400 cm^{-1} , then the difference band, $\nu(\text{OH}) - \nu(\text{L})$, must be observed also. But the "difference" bands corresponding to the bands at 4049 cm^{-1} (2.47μ), 4016 cm^{-1} (2.49μ), and 3788 cm^{-1} (2.64μ) are not observed, hence these three bands cannot be sum combinations.

Moreover, by the above argument, the bands at 4082 cm^{-1} (2.45μ), 3952 cm^{-1} (2.53μ), and 3690 cm^{-1} (2.71μ) cannot be sum bands, because their corresponding "difference" bands are not observed.

The same argument cannot be extended to cover the bands at 4310 cm^{-1} (2.32μ), 4465 cm^{-1} (2.24μ), 4565 cm^{-1} (2.19μ), and 4860 cm^{-1} (2.06μ), since the lattice frequencies necessary to allow these to be sum bands are relatively high (661 cm^{-1} , 816 cm^{-1} , 916 cm^{-1} , and 1211 cm^{-1}), making the corresponding levels from which the difference transitions would originate sparsely populated.

Through the above reasoning, it has been shown that it is most unlikely that an energy level diagram of the type shown in Fig. 25(a) represents the correct origin of the ten absorption bands found in the brucite spectrum at 4082 cm^{-1} (2.45μ), 4049 cm^{-1} (2.47μ), 4016 cm^{-1} (2.49μ), 3952 cm^{-1} (2.53μ), 3788 cm^{-1} (2.83μ), 3690 cm^{-1} (2.71μ), 3649 cm^{-1} (2.74μ), 3533 cm^{-1} (2.83μ), 3268 cm^{-1} (3.06μ), and 3247 cm^{-1} (3.08μ). However, if the proposal of Bernal

and Megaw (see 1.2) that the OH ions are aligned parallel to the c-axis were correct, then the energy level scheme in Fig. 25(a) would be the only one that could account for the complex spectrum in the neighborhood of the OH stretching frequency. That this follows is evident from reviewing the necessary characteristics of the brucite spectrum given in 3.1 should their proposal be correct. One is then forced to the conclusion that their structure determination with regard to the OH ions is incorrect.

The interpretation of the infrared spectrum has lead to the conclusion that there are at least ten OH stretching fundamental frequencies which have different dichroic properties. In order to explain the presence of many OH fundamentals, an energy level diagram different from Fig. 25(a) is required. The simplest alternative is given in Fig. 25(b), in which all transitions originate from the ground state. The separation of each upper level from the level representing the state of a "free" OH ion is a measure of the interaction that occurs among the OH ions in a unit cell for each OH stretching mode. This energy level scheme overcomes the objection raised to the one in Fig. 25(a), because it allows the many OH stretching fundamentals that are observed.

In addition, there is further evidence that supports the scheme proposed in Fig. 25(b). As was shown in Table 4, the bands occurring near 4350 cm^{-1} (2.30μ), 4070 cm^{-1} (2.48μ),

3660 cm^{-1} (2.73μ), and 3260 cm^{-1} (3.07μ) for $\text{Mg}(\text{OH})_2$ appeared near 3080 cm^{-1} (3.25μ), 2920 cm^{-1} (3.43μ), 2680 cm^{-1} (3.73μ), and 2300 cm^{-1} (4.35μ) in the spectrum of $\text{Mg}(\text{OD})_2$, i.e. these absorptions were each shifted by approximately $\sqrt{2}$ to longer wave lengths upon deuteration. The curves in Fig. 26 clearly illustrate this fact. Curve (a) represents the brucite powder spectrum shifted to higher wave lengths by $\sqrt{2}$, and curve (b) is the spectrum of $\text{Mg}(\text{OD})_2$.

The $\sqrt{2}$ shift in wave length is exactly what is predicted for the 4070 cm^{-1} , 3660 cm^{-1} , and 3260 cm^{-1} absorptions according to the interpretation that these are composed of OH stretching fundamentals, i.e. the substitution of deuterium for hydrogen increases the reduced mass of the OH by approximately a factor 2 and hence reduces the stretching frequency by a factor near $\sqrt{2}$.

Had these bands been combinations of an OH stretching fundamental frequency with low frequencies of the Mg-O lattice, then an entirely different shift would have been observed upon deuteration. The central OH band would have shifted by $\sqrt{2}$, but the combination bands would have appeared on either side of the OD band and separated from it by the same amount of wave numbers as was observed for $\text{Mg}(\text{OH})_2$.

The relative intensities among the group of bands near 3.73μ for $\text{Mg}(\text{OD})_2$ is not quite the same as that for

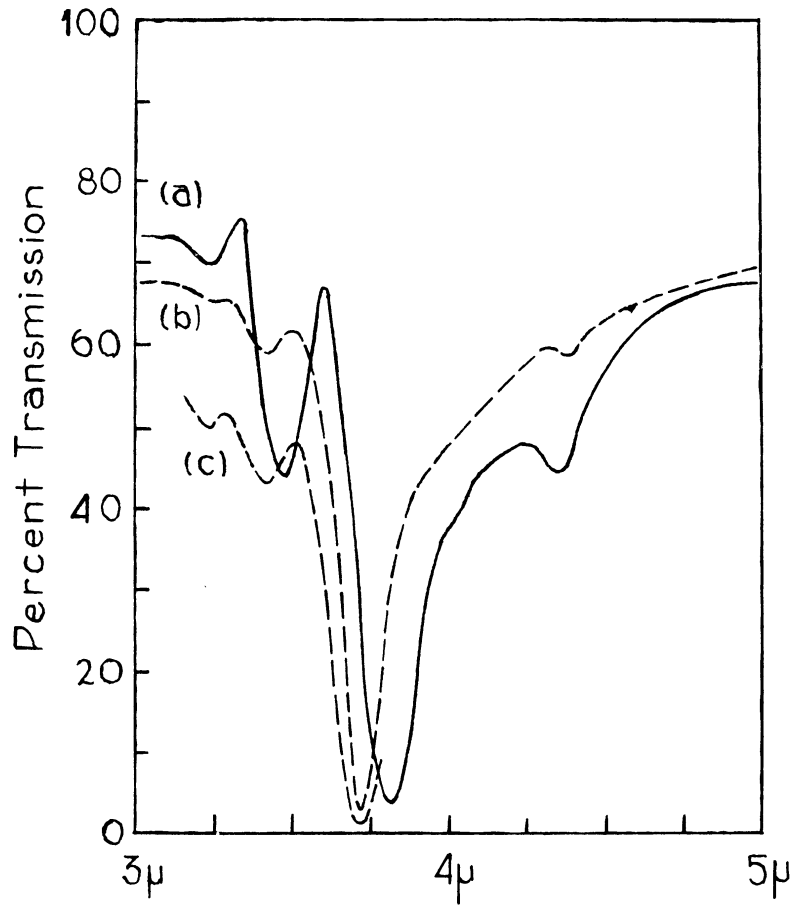


Fig. 26. (a) $\text{Mg}(\text{OH})_2$ Spectrum with each Point on Curve Multiplied by $\sqrt{2}$, (b) and (c) $\text{Mg}(\text{OD})_2$ Powder Spectrum (NaCl).

the bands grouped near 2.73μ for $\text{Mg}(\text{OH})_2$. The central absorption for $\text{Mg}(\text{OD})_2$ near 3.73μ is somewhat stronger relative to the neighboring bands than is the 2.73μ absorption in $\text{Mg}(\text{OH})_2$ (see Fig. 27). Such an occurrence is not surprising, however, since it is impossible at present to predict the functional dependence of the wave function on the mass for each normal mode.

Unfortunately, it was impossible to prepare a deuterated single crystal, and so those bands that correspond to the 2.64μ and 2.83μ bands of $\text{Mg}(\text{OH})_2$ were completely obscured in the spectrum of the deuterated powder. Nevertheless, all the measurements that could be made on the $\text{Mg}(\text{OD})_2$ powder spectrum are in complete accord with the assignment of ten bands as OH stretching fundamental frequencies.

The fact that the 4350 cm^{-1} (2.30μ) absorption also shifted by approximately $\sqrt{2}$ on deuteration is of considerable interest. It will be recalled that we were unable to prove that this absorption was due to an OH stretching fundamental, since it does not follow that if this absorption is due to a sum combination, then the corresponding difference combination must be observed also. The only combination band that would show a $\sqrt{2}$ shift with deuteration is a combination of OH stretching and deformation modes, i.e. $\nu(\text{OH}) + \delta(\text{OH})$. It is not possible from the present evidence to say with certainty whether the above

absorption band is a combination of this type or an OH fundamental, but the former seems a more probable assignment since the latter leads to an extraordinarily high value for an OH fundamental.

One further point should be made concerning combinations of OH stretching and deformation modes. If all the OH ions were oriented parallel to the c-axis of the crystal, then the hydrogen atoms would be moving in a potential with triangular symmetry, i.e. C_{3v} . It can be shown that through first order in all calculable quantities (wave function, energy, selection rule, intensity, etc.), triangular symmetry gives the same results as cylindrical symmetry. Thus, the OH deformation modes would be degenerate, and the concept of in-plane and out-of-plane deformation motions would have no meaning. In this case, only one combination band of the type $\nu(\text{OH}) + \delta(\text{OH})$ can be present in the spectrum. However, if the OH directions are such that the triangular symmetry no longer holds for the deformation motion, then it is possible to have more than one deformation frequency, and hence multiple combinations of the type $\nu(\text{OH}) + \delta(\text{OH})$ may be observed.

We will next discuss the results of the high and low temperature experiments in light of the preceding interpretations. The intensity of an infrared active absorption band is dependent upon the matrix element $\int \psi''^* M \psi' d\tau$ and upon the population of the energy state from which the

associated transition originates. If there is no change of phase, or more precisely, if there is no change in Ψ and Ψ'' , then the variation of intensity with temperature is dependent upon the variation in the population of the lower level with a change in temperature. If a particular temperature change increases the population of a level from which a transition originates, then the intensity of the absorption band associated with that transition will exhibit an increase in its intensity. The converse is of course true, if the temperature change brings about a decrease in the population of the initial level of a transition. An increase in temperature shifts the maximum of the population distribution to higher energy, i.e. higher ν , so that the intensity of a band associated with a transition originating from the ground state, e.g. fundamentals and sum combinations, should not increase with increasing temperature. On the other hand, these same bands should show an increase in intensity when the temperature is lowered. A difference band shows an increase or decrease in intensity with a temperature increase according as the level from which the associated transition originates is above or below the distribution maximum at room temperature.

The high and low temperature spectra given in Figs. 16 and 17 are not consistent with the energy level scheme given in Fig. 25(a) which would describe the complex of

absorptions from 2μ to 3.1μ as a series of sum and difference combinations. Those bands which would have to be sum bands under such a scheme exhibit increasing intensity for elevated temperatures and decreasing intensity for lowered temperatures. This behavior is exactly counter to what is expected for a sum band. Also, the band at 3788 cm^{-1} (2.83μ), which would be assigned as a difference band associated with a transition from a very low level (near 150 cm^{-1}), shows the opposite behavior to that predicted by this interpretation.

The high and low temperature experiments do not confirm the energy level scheme given in Fig. 25(b), but they are not inconsistent with it either. No immediate explanation is available for the intensity variations with temperature in terms of populations of levels. However, if the temperature changes affect the lattice constants of the crystal, and hence the interactions among the OH ions, then one would expect intensity variations that might be more extreme than those due simply to differences in population.

4.3 Summary

The infrared data have been shown to be in conflict with the x-ray structure determination of Bernal and Megaw as far as it concerns the orientations of the hydroxyl ions in the brucite lattice. In contradiction to

what can be predicted for their structure (see 3.1), ten OH stretching fundamental frequencies have been found in the infrared absorption spectrum, at least six of these having components of dipole moment change perpendicular to the c-axis. In addition, these OH stretching frequencies range from 4082 cm^{-1} to 3247 cm^{-1} , so that considerable interaction must take place among the hydroxyl ions in a unit cell.

We now propose a modification of the Bernal and Megaw structure with respect to the OH orientations only, and this will be discussed in the following chapter.

CHAPTER 5

A Suggested New Structure for Brucite

5.1 Demands on the Structure

Since we have discussed the infrared properties of only the hydroxyl ions in brucite, any new structure proposal will deal exclusively with the hydroxyl orientations in the crystal.

It is clear from the foregoing discussion that properties of the infrared spectrum of brucite demand that particular requirements be met by any structure proposal. These are listed below.

(a) All OH ions cannot be oriented parallel to the c-axis. This is required, because the OH stretching modes result in dipole moment changes having components both parallel and perpendicular to the c-axis. The angle between the c-axis and the OH ions has not been fixed, in fact more than one angle may exist.

(b) The unit cell must contain at least ten OH ions. Because if there are n OH stretching fundamental frequencies in the infrared spectrum of a crystal, then there must be at least n OH ions in a unit cell. There may of course be more OH ions to a unit cell than there are OH stretching fundamentals active in the infrared, depending upon how many of the frequencies are mutually exclusive in the infrared and Raman spectra.

(c) The projection of the crystal lattice on a plane perpendicular to the c-axis must have triangular symmetry (or higher). This is necessary, since the OH frequencies exhibit no dichroism when the incident beam is parallel to the c-axis.

(d) There must be considerable interaction among the OH ions. Such interaction must exist, because the OH fundamental stretching frequencies are shifted up to several hundred wave numbers from the "free" OH stretching frequency.

5.2 Suggested OH Orientations

The manner in which many OH stretching frequencies with different polarization properties may arise is illustrated by a simple example. Suppose that there are two OH ions per unit cell and that they are oriented at some angle to the c-axis as shown in Fig. 27(a). Neglecting any deformation motions, the two normal modes associated with OH stretching frequencies are the in-phase and out-of-phase stretching motions shown in Figs. 27(b) and (c). The frequencies corresponding to these two modes are different according as the interactions between the OH ions are different for the two motions. The in-phase mode results in a change of dipole moment parallel to the c-axis, since the perpendicular components cancel. On the other hand, the out-of-phase mode exhibits a dipole moment

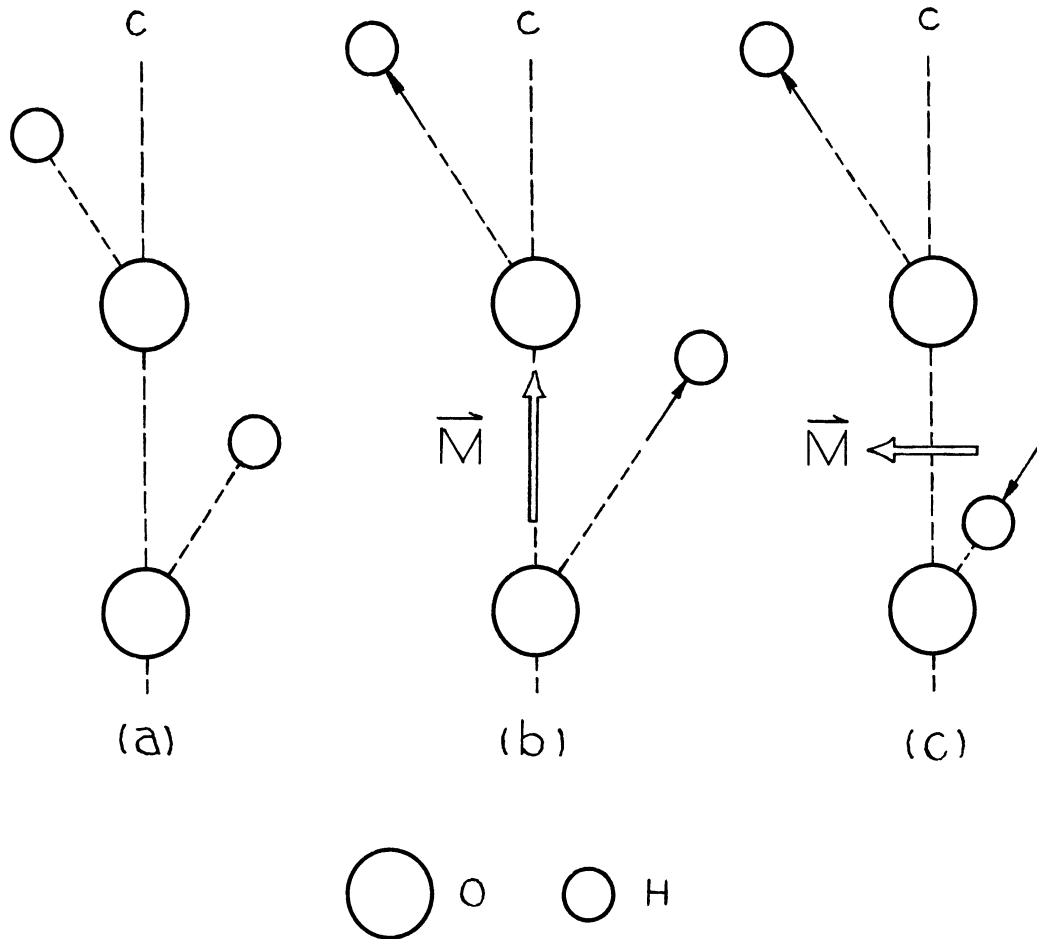


Fig. 27. Example of OH Stretching Modes for a Unit Cell Containing Two OH Ions, (a) Equilibrium Position, (b) In-Phase Mode, (c) Out-Of-Phase Motion.

change normal to the c-axis, the parallel components canceling. In this way, one finds that there are two OH stretching frequencies with opposite polarization properties.

In a similar way, a unit cell with many OH ions can result in many OH stretching frequencies with a variety of polarization properties. With only the present evidence, it is impossible to say with certainty in what manner the OH ions must be oriented in brucite. However, a possible structure that would qualitatively fit the requirements listed in 5.1 is given in Fig. 28.

The hydrogen atoms lie along a line joining the nearest oxygen atoms in neighboring layers. The projection on the (0001) plane is shown in Fig. 28(a), while the projection on a plane normal to (0001) and normal to an a-axis is given in Fig. 28(b). From x-ray diffraction measurements, the parameter of the crystal was calculated to be $u = 0.22$. Using this value, the nearest O-O atoms in neighboring layers are 3.19Å apart. This distance is too great to allow the hydrogen bonding that is shown in Fig. 28. However, in a private communication, H. D. Megaw gave as her opinion that the determination of the parameter could well be in error by as much as ± 0.04 . If the parameter is 0.26, then the O-O distance is only 2.89Å, and hydrogen bonding may occur for such distances.

If the OH ions are oriented as shown in Fig. 28,

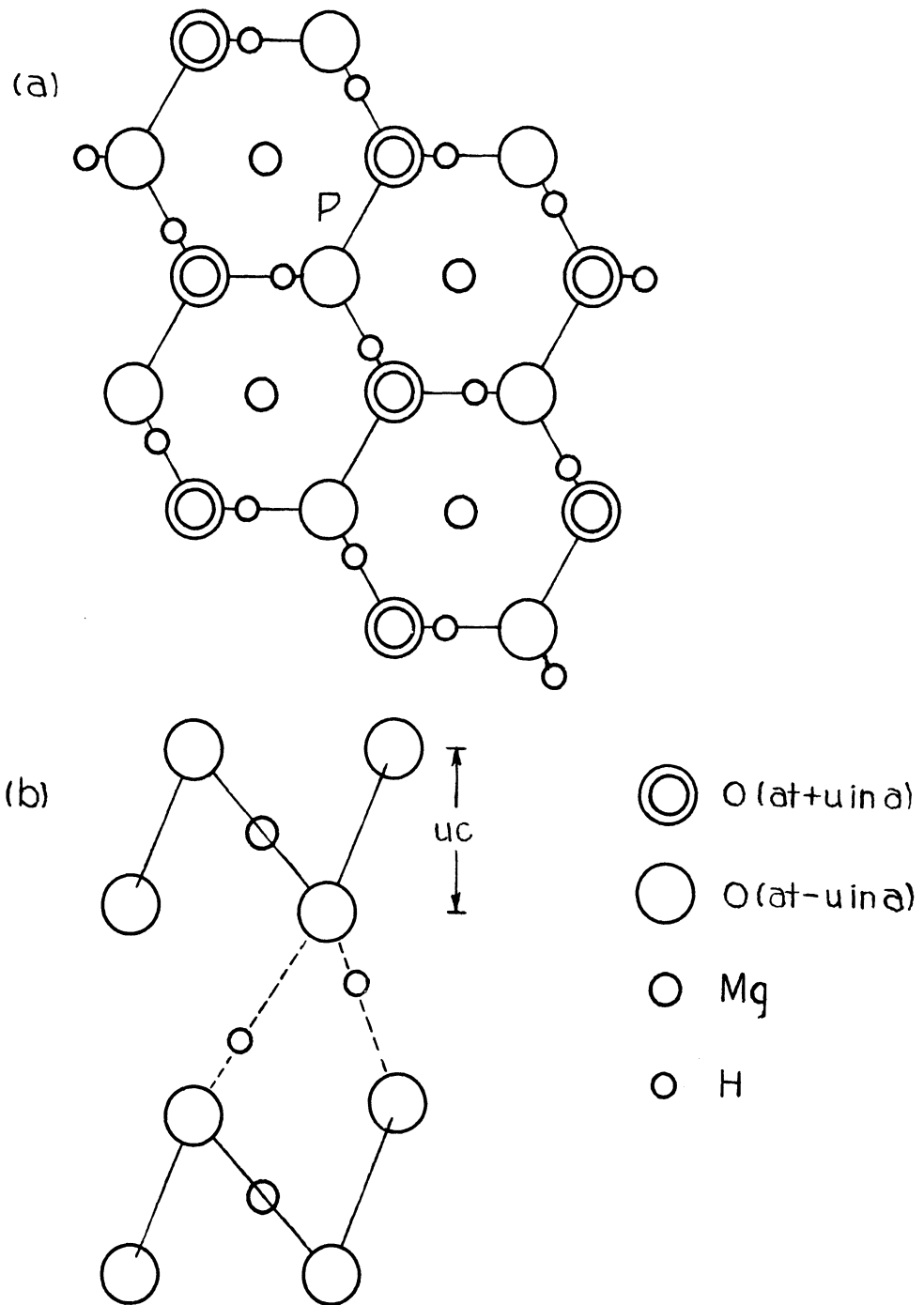


Fig. 28. A Suggested Arrangement of the H Atoms in the Brucite Crystal Lattice, (a) Projection on (0001) Plane, (b) Projection on a Plane Normal to the (0001) Plane and Normal to an a-axis.

then the crystal is only pseudo-hexagonal, i.e. the Mg-O lattice is hexagonal, but this symmetry is destroyed when the hydrogen positions are considered. The unit cell is twice the size of that deduced solely from the O and Mg atoms. The new unit cell would contain four OH ions, which is insufficient to account for the ten OH stretching fundamentals found in the infrared spectrum.

However, one notices that there are three equivalent ways in which the orientations can occur. One of these is shown in Fig. 28(a). The other two are obtained by rotating this diagram 120° and 240° about an axis normal to the page and passing through an oxygen position (e.g. at position P). The results of these operations are shown in Figs. 29(a) and (b). Since the distance between successive regions of hydrogen bonding is approximately 4.73\AA , it is doubtful that the choice of one of these orientations has any effect on the manner in which the successive layers are bonded. This would mean that the three patterns would occur in a random fashion. If this is the case, then there is no true repeat distance along the c-axis of the crystal, and hence there is no unique unit cell. All the consequences of such a structure are not easy to foresee, since three different kinds of "unit cells" of $2\text{Mg}(\text{OH})_2$ would occur in the crystal. Thus, brucite could not be a single crystal at all in the macroscopic sense, but it would simply be a collection of small crystals with slightly varying

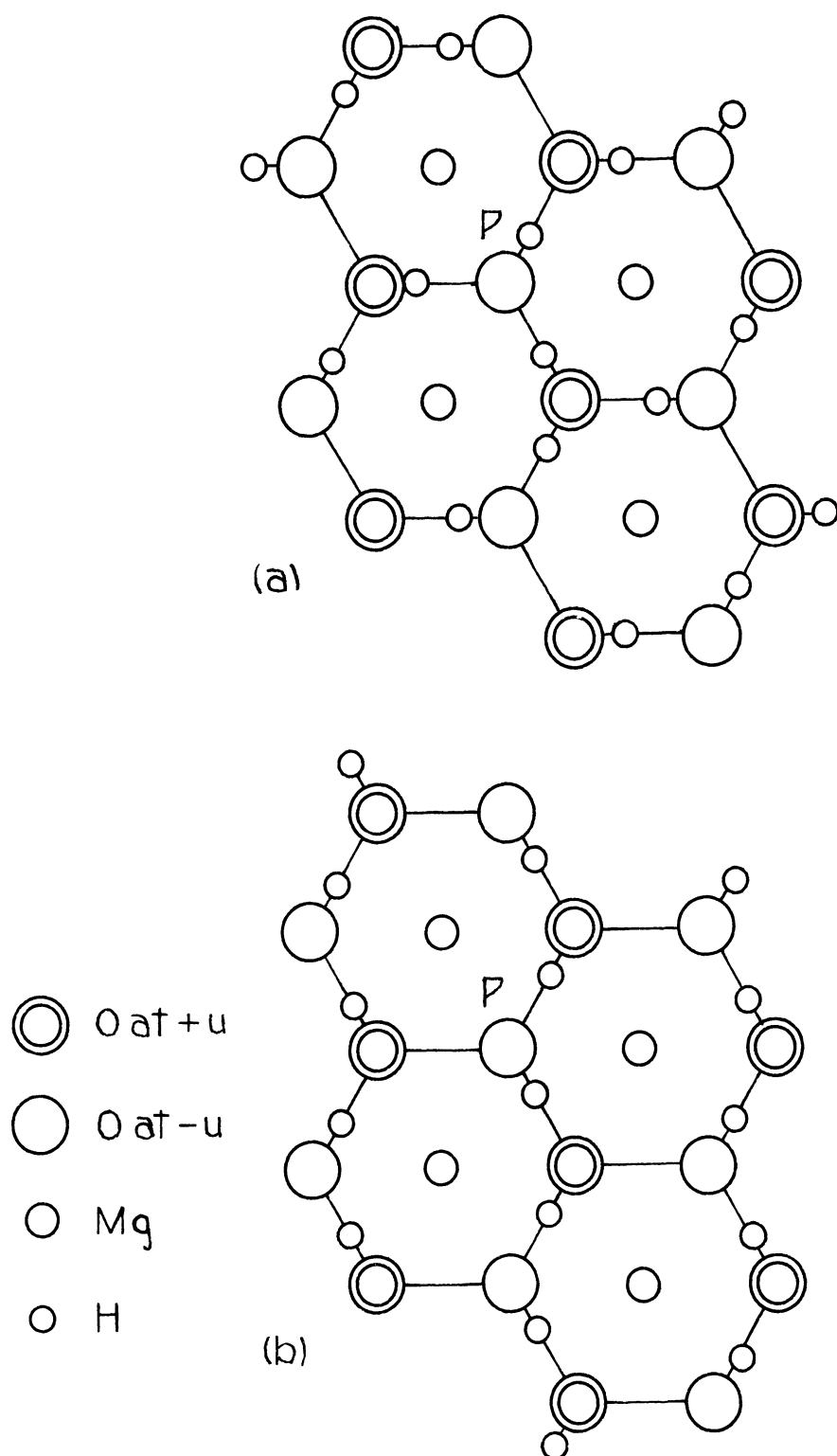


Fig. 29. Alternative Arrangements that are Equivalent to That in Fig. 28(a) Obtained by Rotating by (a) 120° and (b) 240° About the O Atom at the Point P.

unit cells.

This is the point reached in the present investigation of brucite through its infrared absorption spectrum. There are other experiments which might help to prove or disprove the suggested structure. These are listed below.

(a) Knowledge of the Raman spectrum of brucite could help to determine the total number of OH stretching fundamental frequencies by locating those which are infrared inactive.

(b) A re-examination of good brucite crystals by modern x-ray techniques is desirable. A re-evaluation of the parameter U should be made, so that one may be more certain of the OH-OH distances between neighboring layers.

(c) Neutron diffraction work would be of considerable aid in placing the hydrogen atoms in the crystal.

(d) The overtone region between 1μ and 1.6μ should be studied in the infrared with high resolution and with thick samples. The fact that many of the bands in the 2μ to 3.1μ interval do not seem to exhibit overtone bands could be important in assigning their species.

(e) Finally, it might be enlightening to examine the infrared spectra of the other crystals which have the same structure as brucite, e.g. $\text{Ca}(\text{OH})_2$, $\text{Mn}(\text{OH})_2$, $\text{Ni}(\text{OH})_2$, $\text{Co}(\text{OH})_2$, $\text{Fe}(\text{OH})_2$, and $\text{Cd}(\text{OH})_2$. A detailed study of these crystals might lead to a correlation of band positions and intensities

with the dimensions of the crystals and possibly with the nature of the cations. The mineral Gibbsite (or Hydrargillite), $\text{Al}_2(\text{OH})_3$, has the brucite structure⁴⁰ in every layer, but each layer is a mirror image of its neighboring layers, so that the contrast between the brucite and Gibbsite spectra might give additional information.

BIBLIOGRAPHY

1. A. F. Rogers and P. F. Kerr, *Optical Mineralogy*, McGraw-Hill, N. Y. (1942)
2. *Handbook of Chemistry and Physics*, 30th Edition
Chemical Rubber Publishing Co, Cleveland (1947)
3. H. Inudzuka, *J. Geol. Soc. Japan* 48, 244 (1941)
4. W. F. Giauque and R. C. Archibald, *J. Amer. Chem. Soc.* 59, 563 (1937)
5. W. Hankel, *Wied. Ann.* 6, 54 (1879)
6. H. D. Megaw, *Proc. Roy. Soc.* A142, 207 (1933)
7. G. Aminoff, *Geol. Foren. Forh. Stock.* 41, 407 (1919)
8. G. Aminoff, *Z. Krist.* 56, 506 (1921)
9. G. R. Levi and A. Ferrari, *Atti. Luic.* 31, 397 (1924)
10. G. Natti and L. Passerini, *Gazz.* 58, 617 (1928)
11. L. R. Bury and E. R. H. Davies, *J. Chem. Soc.* 2013 (1932)
12. F. Trendelenburg and O. Wieland, *Wiss. Veroffentl. Siemens-Konzern* 13, 37 (1924)
13. J. Garrido, *Z. Krist.* 95, 192 (1936)
14. J. D. Bernal and H. D. Megaw, *Proc. Roy. Soc.* A151, 384 (1935)
15. W. W. Coblentz, *Investigations of Infrared Spectra*, Washington, D. C., Carnegie Institution of Washington, (1905-1908)
16. W. W. Coblentz, *Phys. Rev.* 20, 252 (1905)
17. E. K. Plyler, *Phys. Rev.* 28, 284 (1926)
18. M. Yeou Ta, *Comptes Rendus* 211, 467 (1940)
19. M. Yeou Ta, *Comptes Rendus* 209, 990 (1939)
20. J. Louisfert, *J. Phys. et Rad.* 8, 21 (1947)
21. C. Duval and J. Lecomte, *Bull. Soc. Chim.* 8, 713 (1941);
Bull. Soc. Franc. Mineral 66, 284 (1943)
22. J. Lecomte, *Proc. Indian Acad. Sci.* 28, 339 (1948)

23. A. W. Laubengayer, General Chemistry, Reinhardt and Co. Inc., N. Y. (1949)
24. W. D. Keller and H.E. Pickett, Amer. J. Sci. 348, 264 (1950)
25. E. Hasche, Ann. der Phys. 8, 59 (1931)
26. J. U. White and M. D. Liston, J. Opt. Soc. Amer. 40, 29, 93 (1950)
27. E. F. Barker and E. A. Boettner, Instruction Manual for the Double Beam Source Unit of the University of Michigan Infrared Spectrometer (1951)
28. A. Walsh, Nature 167, 810 (1952)
29. H. B. Kessler, Thesis, University of Michigan (1953)
30. A. Vallance-Jones, Thesis, Cambridge, (1949)
31. J. M. Hunt, M. P. Wisherd, and L. C. Bonham, Anal. Chem. 22, 1478 (1950)
32. R. E. Rundle and M. Parasol, J. Chem. Phys. 20, 1487 (1952)
33. R. C. Lord and R. E. Merrifield, J. Chem. Phys. 21, 166 (1953)
34. S. Bhagavantam and T. Venkatarayudu, Proc. Indian Acad. 9A, 224 (1939)
35. R. C. Halford, J. Chem. Phys. 14, 8 (1946)
36. D. F. Hornig, J. Chem. Phys. 16, 1063 (1948)
37. R. G. Wyckoff, Crystal Structures, Interscience
38. G. Herzberg, Spectra of Diatomic Molecules, D. Van Nostrand Co., New York (1950)
39. G. Herzberg, Infrared and Raman Spectra, D. Van Nostrand Co., New York, (1945)
40. H. D. Megaw, Z. Krystallog. 87, 185 (1934)

